University of Groningen

Bachelor Research Project

A comparative analysis on Lattice QCD determined decay properties in $B^+ \to \tau^+\nu_\tau$ and $B_c^+ \to \tau^+\nu_\tau$

Student:
Prerna Sarkar *(s4715349)*

Supervisor:
Kristof de Bruyn

1 Abstract

This comparative analysis considered the Lattice QCD determined decay properties of the leptonic decay modes $B_{(c)} \to \tau^+\nu_\tau$ in the form of a literature review. Although the LQCD determined mass of B^+ is expected to be more precise than that of B_c^+, due to the latter having errors associated to it that are absent or smaller for B^+, the results presented in ref. [1] and ref. [2], don't reflect this. The decay constants presented in ref. [2], [3], [4] and [5] indicate a smaller uncertainty for B^+ than for B_c^+, matching expectations. The determination of the meson masses and decay constants primarily utilized techniques incorporating NRQCD valence b quarks in combination with HISQ u/c quarks and techniques incorporating only HISQ valence quarks. With these decay properties, as well as the relevant CKM matrix elements and experimentally determined parameters such as the mesons lifetimes (due to these not being determined through LQCD yet), the branching fractions of the subsequent decay modes were calculated to be: $\mathcal{B}(B^+ \to \tau^+\nu_\tau) \approx 0.99(6) \cdot 10^{-4}$ and $\mathcal{B}(B_c^+ \to \tau^+\nu_\tau) \approx 1.92(6) \cdot 10^{-2}$. The largest contributions towards the branching fractions uncertainties are relevant the CKM matrix elements $|V_{ub}|$, $|V_{cb}|$ and the decay constants. This paper also gives insight into the less apparent classification of the B_c^+ meson within the heavy-light and heavy-heavy meson families by evaluating the positioning of its decay constant ratio within those of the corresponding meson groups.

Contents

2 Introduction

The ancient question: *What are we made of?* has stirred scientists to study physical phenomena occurring at the smallest of distances. When unravelling the structure of matter, the scientific community established the Standard Model (SM): a theory which forms the cornerstone of particle physics, explaining all but one of the fundamental forces of nature.[1] Starting out as a model for quantum electrodynamics and having evolved to include quantum chromodynamics (QCD) as well as weak interaction effects (such as parity- and CP-violation) [6], the Standard Model currently describes the outcomes of hundreds of thousands of experiments [7].

Powerful as it is, it remains incomplete[2], necessitating the search for Beyond the Standard Model (BSM) physics. The LHCb - an experiment at CERN dedicated to the investigation of rare decays in the charm and beauty sector (among other things) - performs high precision collisions, whose discrepancies from the SM hint at new physics[9]. The clean leptonic decays $B^+ \to \tau^+\nu_\tau$ and $B_c^+ \to \tau^+\nu_\tau$ are in this aspect very interesting. The parent mesons B^+ and B_c^+ are relatively heavy type of hadrons (when compared to the familiar protons and neutrons making up most of the matter in the Universe), composed of a bottom antiquark and lighter other quark: $(\bar{b}u)$ for B^+ and $(\bar{b}c)$ for B_c^+. The interest in their leptonic decays can be justified by, for example, data indicating violations in lepton flavour universality (LFU) [10]. LFU states that the coupling of leptons to the electroweak force is independent of the flavour of the lepton taken in consideration (whether it is $e^\pm, \mu^\pm$, or $\tau^\pm$)[11]. The B^+ case is evaluated with the upper limit on the branching ratio of the $B^+ \to e^+\nu_e$ and $B^+ \to \mu^+\nu_\mu$ decays. The upper limit indicates the maximum probability of the relevant decay mode to occur compared to all possible decays and is used since the rates for decays to e and μ have not yet been measured. Since the $B_c^+ \to \tau^+\nu_\tau$ has not been observed experimentally, the violation in LFU for this case is recognized with data presenting preferences for lepton flavours when comparing the decays $B \to D^{(*)}\tau\nu_\tau$ and $B \to D^{(*)}l\nu_l$ (with $l = e, \mu$). This is permissable because these decays are mediated by the same quark-level process ($b \to cl\nu_l$) as the one mediating $B_c^+ \to \tau^+\nu_\tau$[12].

However, besides being enticing probes for BSM effects, the decays $B^+/B_c^+ \to \tau^+\nu_\tau$ also test a crucial Standard Model feature: the CKM matrix elements $|V_{ub}|$ and $|V_{cb}|$ respectively. Together with the decay constants f_{B^+} and $f_{B_c^+}$ (which quantify the decay probability and are determined through Lattice QCD [13]), they form the main sources of uncertainty in the theoretical determination of the branching fractions [12]. Acquiring precise experimentally obtained branching fractions of these decays has therefore gathered recent interest, also for possibly playing a role in solving the inclusive vs. exclusive puzzle [14].

Unfortunately, observing the $B_c^+ \to \tau^+\nu_\tau$ decay is very challenging at current particle colliders. In hadron colliders, such as the LHCb, this is due to the struggle of separating the decay signal from the overwhelming background noise[3] while the clean environments of current e^+e^- B-factories -such as at Belle II commissioned at SuperKEKB [18]- don't operate at energies of the production threshold of the B_c^+ meson. In this aspect, the $B^+ \to \tau^+\nu_\tau$ decay, determined to have a measurement precision of 20 percent at B-factories [13], is more familiar and well-known than the $B_c^+ \to \tau^+\nu_\tau$ decay. Also regarding the classification of each decays' parent meson, it is clear that a significant divide in knowledge remains: B^+ clearly exhibits characteristics associated to the heavy-light meson group, in which mesons are composed of a heavy quark and light quark, while the classification of B_c^+ —whether it belongs to the heavy-light or heavy-heavy group— is not so obvious. This paper investigates if certain properties, such as the mass, decay constants and branching fractions of the B_c^+ parent mesons decay are less-known than that of its fellow beauty meson, and to what extent this is the case if determined theoretically through LQCD.

This paper starts with an overview of the Standard Model to provide the theoretical framework for understanding the concepts, assumptions and processes relevant to the decays and particles in question. This is followed by a section dedicated to Lattice QCD, which is a non-pertubative model that approximates how the quantum fields of quarks evolve over the course of a strong force interaction by discretising spacetime. In doing so, physical observables and quantities can be extracted using various approaches. Three of these

[1] Gravitational interactions are not accounted for in the Standard Model.

[2] For example, the Standard Model does not offer an explanation for dark matter or integrate neutrino masses, imperative to describe the phenomenon of neutrino oscillations[8].

[3] Although, researchers of the LHCb Collaboration have remarkably managed to observe decays with the B_c^+ as its parent meson numerous times [15][16][17].

are elaborated on in this section, due to their significance and applicability to the heavy quarks in question: The Non-Relativistic QCD (NRQCD) formulation is namely able to address the non-relativistic nature of the b quarks present in both B^+ and B_c^+, while the Highly Improved Staggered Quark (HISQ) discretises the heavy quark fields in such a way that extrapolated values are not accompanied by the traditionally large discretisation errors, substantially improving their precision. The Heavy Quark Effective Theory (HQET) in turn simplifies the treatment of the quarks within the lattice framework by accurately encapsulating the workings of the complex physical system in an approximate effective field.

As such, these techniques (and combinations of them) are utilized in the LQCD determinations of the B^+ and B_c^+ masses and decay constants, which in turn will be used for the determination of their SM branching fractions, which assess the probability of a parent meson decaying via a particular decay mode. The LQCD section will also provide a brief outline of the largest contributing physical effects that are often not taken into account in LQCD calculations (one of them being the effects of electromagnetism) and the method of incorporating them in the extrapolated values. Due to these effects overall contributing more to the B_c^+ meson than for the B^+, as well as the c quark within B_c^+ having larger associated discretisation errors than B^+'s lighter u quark in the utilized HISQ approach, it is expected that the mass and decay constant of B_c^+ will have larger associated errors to them than those of B^+. However, in the case of the SM branching fractions (for which the CKM matrix elements and decay constants are the main sources of uncertainty), this statement can not be made, since the B^+ decay is known to have a larger relative uncertainty corresponding to its CKM matrix element, but expected to have a smaller one for its decay constant. Therefore, a section is dedicated to evaluate the contributions of the relative uncertainties corresponding to decay properties needed to determine the branching fractions of the leptonic decay modes $B^+/B_c^+ \to \tau^+\nu_\tau$. Lastly, the conclusions of this paper are formulated by reflecting on the process and determination of the decay properties discussed.

3 The Standard Model

The Standard Model is written in the language of quantum field theory (QFT), which states that all elementary particles in the Universe are in fact not particles (though often can be approximated as such), but rather oscillations of (relativistic) quantum fields[7], whose properties are governed by the laws of symmetry[19]. Quantum Electrodynamics (QED) in turn predicts the behaviour of particles for one such field: the electromagnetic field, by describing the behaviour of charged particles and photons. In fact, the discovery of QED is arguably the first stage of the rapid development of the Standard Model. Over the decades, the Standard Model incorporated the strong force in the form of QCD, the weak force and even formulated the electroweak theory, in which the force carrying particles of QED and the weak force are simultaneously built into. To elaborate on this, the Standard Model predicts that all phenomena in the Universe are the consequence of either matter particles, which carry half-integer spin and compose the group of *fermions*, or force-carrying particles, which carry integer spin and compose the group of *bosons*. Pauli's exclusion principle forms the distinction between these two groups, by stating that only bosons are allowed to occupy the same quantum state, while fermions are forbidden to [7].

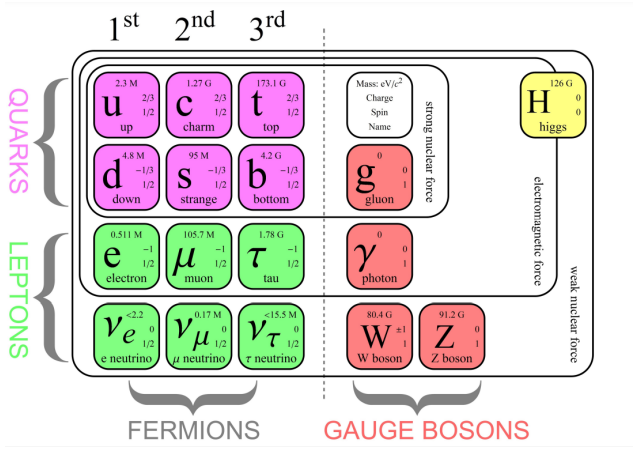

Figure 3.1: Particle content of the Standard Model [20].

3.1 Fermions, Bosons & the Fundamental Forces

The group of fermions, in turn, can be divided into quarks and leptons, as indicated in figure 3.1. The well-known electron e^- falls within the latter group, having two much heavier copies, known as the muon and the tau leptons (μ^-, τ^- respectively). Each lepton has a corresponding neutrino (ν_e, ν_μ, ν_τ), which is neutral and interacts weakly with matter, making it very challenging to detect. The last constituents of the lepton group are the leptons anti-particles; particles with identical inherent properties (such as mass and spin), but with opposite electric charge.

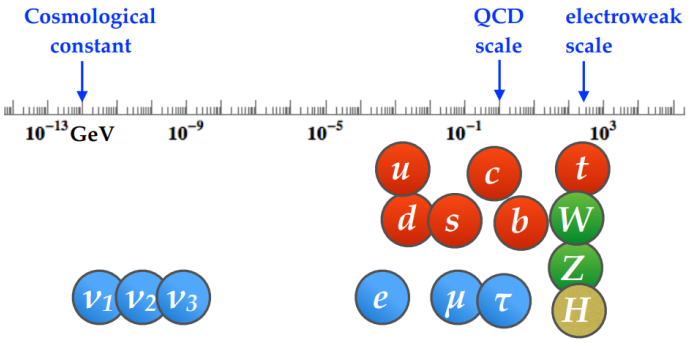

Figure 3.2: The quarks in the 1^{st} generation (u, d) are *light* quarks while those in the 3^{rd} generation (t, b) are classified as *heavy*. The 2^{nd} generation, with quarks having rest masses in between those of the heavy and light quarks in an inexplicable hierarchical structure, doesn't have a distinct label in this manner. This peculiar distribution is the SM flavour puzzle or the flavour hierarchy problem [21].

The group of quarks have a set of corresponding anti-particles also, defined in the same manner. Quarks are the fundamental particles that make up most of the matter in the universe, including protons and neutrons. Just like the group of leptons, there are three generations of quarks, which are ordered based on increasing mass. Besides being the only set of known particles that undergo all of the three fundamental forces included in the Standard Model, quarks also have a fascinating intrinsic property called colour, which dictates much of their behaviour and clarifies the naming of the theory of the strong force: Quantum chromodynamics (QCD). One property of this theory dictates that quarks are not allowed to exist on their own due to colour confinement, in which particles are required to be colour neutral. This effect is so unviolated that, when an attempt is made to separate quarks, it is more energetically favourable for each quark to create a corresponding anti-quark pair (such that together they are colour neutral) than to allow quark isolation to occur.

The naming of composite particles (hadrons) is dependant on the number of quarks composing them. It is important to note here that at the high energies relevant to the processes in this paper, it is oftentimes too much of a simplification to consider hadrons to be composed of just a small number of quarks. The internal structure of a hadron is a chaotic turmoil, with quark anti-quark pairs flying in and out of existence due to gluon annihilation and the possibility of discovering internal quarks heavier than the mass of the hadron its composing (though admittedly this possibility is very small due to the energy-time uncertainty principle $\Delta E \Delta t \geq \frac{\hbar}{2}$)[4]. If one were to take a look at the composition of the internal structure of the hadron at one instant, it will most likely be different than the structure an instant later. This described pandemonium of quarks within a hadron is known as the *quark sea*. All the quark anti-quark pairs within the quark sea at one instant in time should cancel out, besides a few quarks we refer to as the *valence quarks*. Valence quarks have quantum field amplitudes that contribute the most to the apparent structure of the hadron, thus determining its mass, spin, electric charge and momentum. As such, a hadron having two valence quarks (compelled to be a quark and anti-quark due to color confinement) is labeled a *meson*.

The three forces described by the Standard Model are the result of the force-carrying particles named bosons, such that every one of the fundamental forces has a boson associated to it. The most familiar boson is the massless photon γ, the mediator of the electromagnetic force. The strong force has a massless boson called the gluon g associated to it, while the weak force has three massive bosons: the charged W^+, W^- and the neutral Z^0. The mass of the $Z^0, W^\pm$ bosons is a result of a coupling to the Higgs field.

The interaction between particles mediated by all the mentioned forces is often easily explained by the exchange of virtual bosons, leading to the effect of an observable force. In the same way that the electron creates an electromagnetic field that spreads radially outward in space[5], quarks create a gluon field whose strength is also correlated to distance. In the context of the strong force however, the field strength increases with quark distance. This is due to the behaviour of gluons: they create flux tubes between quarks, analogous to a string that can/has been stretched. The strong coupling constant α_s thus increases with quark distance (explaining the creation of anti-particles at attempts of quark isolation) and decreases with energy scales ($\alpha_s \propto 1/q^2$). When α_s is around the order of 1 (at high energy scales and short quark distances), asymptotic freedom is acquired, allowing for the system to be described with help of *pertubative theories*. Pertubative theories approximate the dynamics of the intricate system of hadrons by utilizing expansions of $1/\alpha_s$, analogous to the manner that charged particle interaction strength with the electromagnetic field (as described by Feymann diagrams) decreases by a_{EM} per vertex [23].

However, the most mysterious of all forces described by the Standard Model is undoubtedly the weak force, which dictates the process of decay. It allows for *parent particles*, which are the particles on the left of the Feynman diagram, to decay into *decay products*. This force has many peculiarities, such as the violation of charge and parity conservation[6] and the breaking of flavour symmetry, allowing for phenomena such as neutrino oscillations and quark decay. The relevant decays $B^+/B_c^+ \to \tau^+\nu_\tau$ are mediated by the flavour changing quark level processes $b \to u\tau\overline{\nu_\tau}$ and $b \to c\tau\overline{\nu_\tau}$ respectively.

[4] An example of this phenomenon is finding charm quarks ($m_c = 1.27GeV$) withing the proton ($m_p = 0.94GeV$) one percent of the time. [22]

[5] The electron thus interacts stronger with charged particles situated more closely to it than more distant ones.

[6] The charge conservation symmetry breaking suggests that processes undergoing the weak force need not behave the same when replacing all particles by their anti-particles, while the parity symmetry breaking indicates that the weak force acts upon left handed particles, while not doing so for a spatially inverted system containing right handed particles.

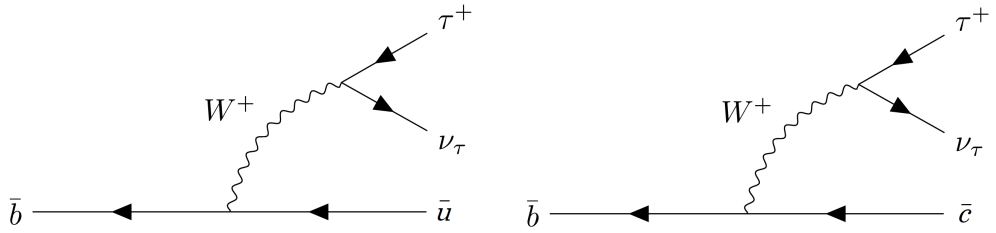

Figure 3.3: Diagrams of the quark level processes that mediate the $B^+/B_c^+ \to \tau^+\nu_\tau$ decays respectively.

3.2 Branching fractions

Branching fractions quantify the probability of a particle decaying via a particular decay mode by evaluating the partial decay fraction of that particle relative to all its possible decay modes. These branching fractions can be experimentally determined, but can also be predicted with theoretical models that are based on internal processes and interactions. In the case of our leptonic decay modes, the branching fractions can be determined with the Standard Model prediction [12]:

$$\mathcal{B}(B_q^+ \to \tau^+\nu_\tau)^{SM} = \tau_{B_q^+} \frac{G_F^2 |V_{qb}|^2 f_{B_q^+}^2 M_{B_q^+} M_\tau^2}{8\pi} (1 - \frac{M_\tau^2}{M_{B_q^+}^2})^2 \tag{3.1}$$

Here $q = u, c$ for the B^+ and B_c^+ respectively. $\tau_{B_q^+}$ denotes the relevant meson lifetime. This quantity contributes positively towards the branching fraction due to it indicating the stability of the parent meson: the longer the lifetime of the parent meson, the higher the possibility for decays to occur, in turn increasing the branching fraction proportionally. The same can be said for the mass of the parent meson $M_{B_q^+}$. The phase space available for this decay is namely dependant on the mass of the parent meson. A higher $M_{B_q^+}$ would thus result in more phase space being available for decay products, increasing the branching fraction. The M_τ^2 and $(1 - \frac{M_\tau^2}{M_{B_q^+}^2})^2$ terms also account for the phase space available, by regarding the difference in mass between the parent meson (B_q^+) and the only massive decay product[7] (τ^+). The G_F denotes the Fermi constant, which indicates the coupling strength of the weak force. $|V_{qb}|$ denotes the relevant exclusive CKM matrix element(3.3), while $f_{B_q^+}$ is the parent mesons decay constant (3.4), which is a quantity related to the weak force determined through Lattice QCD (4). The uncertainty of these latter two variables are expected to contribute the most towards the uncertainty of the branching fraction of these decay modes [24].

3.3 CKM Matrix

The Cabibbo-Kobayashi-Maskawa matrix is a unitary 3×3 matrix which incorporates information about the strength of the weak interaction coupling to individual quarks and in turn their quark level decay probability.

$$V_{CKM} = \begin{pmatrix} V_{ud} & V_{us} & V_{ub} \\ V_{cd} & V_{cs} & V_{cb} \\ V_{td} & V_{ts} & V_{tb} \end{pmatrix}, \tag{3.2}$$

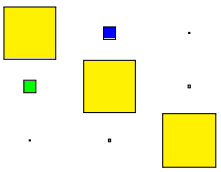

The matrix elements V_{ij} represent the probability of the quark level decay j to i (via a $W^\pm$ boson). The elements that contribute most are along the diagonal, which correspond to processes that don't undergo flavour mixing. The non-zero off-diagonal elements indicate that flavour mixing does occur, however at significantly smaller amplitudes. The decays $B^+/B_c^+ \to \tau^+\nu_\tau$ are sensitive to the matrix elements $|V_{ub}|$ and $|V_{cb}|$ respectively. The extraction of the values of these elements require considering multiple (in the case of the exclusive determination) or all (in the case of the inclusive determination) possible final decay states [8].

[7] The SM predicts the mass of neutrinos to be zero. This is an incorrect prediction, due to the observed phenomena of neutrino oscillations in which propagating neutrinos evolve different flavours over time and must thus experience time, forbidding them to be massless. Equation 3.1 is, however, a standard model prediction, in which the neutrino is massless.

[8] The exclusive and inclusive measurements contradict each other, with the inclusive values always being determined to be significantly larger than the exclusive values, despite theory predicting them to coincide. This tension has lead to the longstanding inclusive vs. exclusive puzzle [14].

This comparative analysis only considers one final decay state (namely that of the $\tau\nu_\tau$), and therefore the values of these CKM matrix elements are taken from literature, instead of determined in this paper. The values of these matrix elements extracted through B meson decays have been determined to be [25]:

$$|V_{ub}|_{excl.} = 3.51(12) \cdot 10^{-3}, \quad |V_{cb}|_{excl.} = 39.10(50) \cdot 10^{-3} \tag{3.3}$$

These values have been determined by using a combination of studying the rate of certain decays and imposing theoretical constraints such as the relevant form factors, which are quantities that describe the internal structure of hadrons when undergoing interactions with other particles. The subscript *excl.* in equation 3.3 indicates that these values represent the exclusive CKM matrix elements of $|V_{ub}|$ and $|V_{cb}|$. These are chosen for the determination of the branching fraction (instead of the inclusive measurements), since they reflect the dynamics of our specific decay channels better than the inclusive elements which sum over all possible decay channels of very diverse dynamics. Since the exclusive matrix element also employs form factors, which are often determined utilizing the same kind of methods as other quantities in this paper, this choice ensures consistency and compatibility with the remainder of the theoretical framework.

3.4 Decay constant

Since the values of the relevant CKM matrix elements will not be determined in this paper, the focus of this analysis shifts now to the decay constants, due to their significant contribution towards the uncertainty of the branching fractions of the leptonic decay modes.

Decay constants, denoted as f_P, are singular values that indicate the interaction strength of the corresponding meson with the weak force, parameterising the probability of the meson annihilating to a W boson [3]. They are inherent to the meson[26] and, when considering B_q mesons (where $q = u, d, s, c$), they are represented by the matrix element of the local current that causes the meson to annihilate [3]. This matrix element represents the overlap of the meson state with the vacuum state through the weak force and is thus dependant on the interaction strength that binds the quarks within the meson. The local current differs for pseudoscalar and vector mesons, being a temporal axial current J_{A_0} for pseudoscalars and a spatial vector current J_{V_i} for vector mesons. Their respective relation to the decay constant is [3]:

$$\langle 0|J_{A_0}|P\rangle = f_P M_P \tag{3.4}$$

$$\left\langle 0\middle|J_{V_i}\middle|P_j^*\right\rangle = f_{P^*} M_{P^*} \delta_{ij} \tag{3.5}$$

Here P represents a pseudoscalar B_q meson and P^* its vector meson counterpart, while $M_{P^{(*)}}$ is simply the mass of the meson in question. The temporal axial current J_{A_0} is defined as [4]:

$$J_{A_0} = (1 + \alpha_s z_0)(\langle J_0^{(0)}\rangle + (1 + \alpha_s z_1)\langle J_0^{(1)}\rangle + \alpha_s z_2 \langle J_0^{(2)}\rangle) \tag{3.6}$$

where α_s is the strong coupling constant and z_i are renormalization coefficients for the pertubative matching of the corresponding axial vector current [4], causing, for example $z_1\alpha_s$ to be a radiative correction to the current $J_0^{(1)}$ [3]. Assuming these corrections to be small (which is relatively precise, particularly in the case $q = l$ [3]), the axial current J_{A_0} described in 3.6 can be simplified to:

$$J_{A_0} = (1 + \alpha_s z_0)(\langle J_0^{(0)}\rangle + \langle J_0^{(1)}\rangle) \tag{3.7}$$

The terms $J_0^{(i)}$ are current operators composed of light quark fields ψ_q and heavy quark fields ψ_Q in the following manner:

$$J_0^{(0)} = \overline{\psi}_q \gamma_5 \gamma_0 \psi_Q, \quad J_0^{(1)} = -\frac{1}{2m_b} \overline{\psi}_q \gamma_5 \gamma_0 \gamma \cdot \psi_Q \tag{3.8}$$

Here $\overline{\psi}_q$ is the Dirac adjoint of the light quark field, defined as: $\overline{\psi}_q = \psi^\dagger \gamma_0$, γ_5 is the fifth gamma-matrix (which is closely related to chirality) and γ_0 the time component gamma-matrix [27]. The incorporation of these gamma matrices is due to the fact that these currents are required to be invariant under Lorentz transformations, causing them to be bilinear covariants which have the preceding form [28].

Utilizing a multi-exponential Bayesian fit function [29] (which will be touched upon in more detail in section 6.3), the amplitudes of $J_0^{(i)}$ can be extracted through Lattice QCD simulations (4):

$$A_{A_0} = \frac{\langle 0|J_0^{(0)}|P\rangle}{\sqrt{2M_P}}, \quad A_{A_1} = \frac{\langle 0|J_0^{(1)}|P\rangle}{\sqrt{2M_P}} \tag{3.9}$$

Combining this with equations 3.4 and 3.7, we find an expression for the decay constant of a B_q pseudoscalar meson (multiplied by the square root of its mass) expressed in amplitudes of the axial currents:

$$f_P\sqrt{M_P} = (1+\alpha_s z_0)(A_{A_0}/\sqrt{2} + A_{A_1}/\sqrt{2}) \tag{3.10}$$

3.4.1 Decay constant ratio's

Since decay constants encompass information on the mesons internal structure, an insightful property to investigate regarding mesons and their stability is the decay constant ratio of the vector and pseudoscalar meson, defined as follows [3]:

$$R_q = \frac{f_{P_q^*}\sqrt{M_P^*}}{f_{P_q}\sqrt{M_P}} = (1+\alpha_s(z_{V_i} - z_{A_0}))\frac{A_{V_0 i} + A_{V_1 i}}{A_{A_0} + A_{A_1}} \tag{3.11}$$

4 Lattice QCD

When the strong coupling constant α_s becomes very high at large quark distances and low energy scales (low q^2) the non-pertubative scale of the strong interaction is attained: Λ_{QCD}. Beyond this energy, pertubative theories (which utilize expansions in $1/\alpha_s$) fail. This is due to the interactions between the quark and gluon fields being so intense under these circumstances that they can not be approximated by virtual particles anymore and so Feynmann diagrams as well as the concept of virtual particles must be discarded. We require an adapted theory to simplify the intricate behaviour of hadrons[23], guiding us to the non-pertubative theory of Lattice QCD.

4.1 Working Principle

Lattice Quantum Chromodynamics (LQCD) is a model that approximates how the quantum fields themselves evolve over the course of a strong force interaction. The starting point in this model is the assumption that time is another dimension of space. Analogous to the Feynmann path integral (in which one evaluates all possible paths between two points in physical space), Lattice QCD evaluates the possible "paths" between two space-time field configurations. This is mathematically equivalent to [30]:

$$\langle\psi_f(t_f)|\psi_i(t_i)\rangle = \int D\psi(t)e^{-S(\psi)} \tag{4.1}$$

where $\langle\psi_f(t_f)|\psi_i(t_i)\rangle$ is the transition amplitude between two space-time configurations, while $\int D\psi(t)e^{-S(\psi)}$ is a functional integral over all possible configurations evaluated at the Euclidean time and restrained by the exponent of the action S, defined as:

$$S(\psi) \equiv \int_{t_i}^{t_f} \delta t L(\psi, \dot{\psi}) \tag{4.2}$$

When doing this, one is faced with two infinities: the infinite evolution possibilities of field oscillations between initial and final configuration *and* the infinite points contained within the fragment of space-time taken into consideration. The first is dealt with Monte Carlo sampling, which is a method which utilizes a random selection from a distribution. For this, a set of values of $\psi_j, j = 0, 1, ...N$ is taken, called a configuration. The configurations with largest $e^{-S(\psi)}$ values contribute most to the integral. Through a process called importance sampling, configurations with probability of $e^{-S(\psi)}$ are generated, for minimal variance and maximum efficiency. Utilizing this method results in a statistical error associated to the determined value of the observable [30]. The second infinity is dealt by pixelating space and time [23]. This, in turn, is done by discretising time: $t_j = t_i + j \cdot a$, where a is the lattice spacing defined as:

$$a \equiv \frac{(t_f - t_i)}{N} \tag{4.3}$$

This is actually what caused $\psi(t)$ to become $\psi_j, j = 0, 1, ...N$ (discretising it also), with the requirement that it must be evaluated over all its indices. Equation 4.1 thus becomes:

$$\langle\psi_f(t_f)|\psi_i(t_i)\rangle = A\int_{-\infty}^{\infty} \delta\psi_0\delta\psi_2...\delta\psi_{N-1}e^{-S(\psi)} \tag{4.4}$$

Here A is a normalisation constant and $S(\psi) = \sum_{j=0}^{N-1} L(\psi_j, \dot{\psi}_j)$. The action of discretising space-time results in a four-dimensional lattice of points -which represents the quark field- with connections that represent the gluon field [23].

Lattice QCD calculations of physical observables or quantities (such as for example the masses of quarks within a meson or their decay constants) require multiple simulations on the lattice, each measuring the value of the observable or quantity for different lattice spacings. This is due to the fact that the values of observables and quantities determined through LQCD are dependant on lattice spacing, with their values being more accurate with decreasing lattice spacing (while their true value arises when the lattice spacing $a = 0$, mimicking real-life physical systems). This can be observed in figure 4.1 as well as in equation 4.4 by registering that the integral is only accurate for large N and thus (due to the definition of a) small lattice spacing. Small lattice spacings, however, come at the cost of large computational power, such that LQCD simulations for investigating properties of light and heavy mesons usually utilize lattice spacings a between $0.06fm$ and $0.15fm$ [31]. By analyzing the trend between the lattice spacing a and the corresponding values of the desired observable, one can extrapolate the true value of the observable at zero lattice spacing. Discretising space-time, however, results in discretisation errors, which are proportional to a in many approaches, such that the value of the determined observable is accompanied by both a statistical and discretisation/systematic error.

Another noteworthy aspect of LQCD simulations is that an artificial frequency cut-off in the UV region (to discard infinities that arise from high momentum particles) is not necessary. This is because a cut-off emerges naturally due to the fact that wavelengths lower than a (corresponding to particles with momenta higher than π/a) are automatically disregarded, since they are not detected in the lattice.

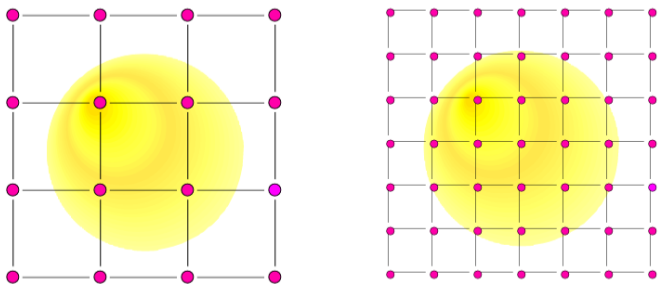

Figure 4.1: A particle on two different lattice spacings, having a more accurate length scale in the presence of lower a. It can also be envisioned that particles associated with wavelengths less than a will not even correspond to a measure of available lattice spacing and thus a natural cut-off is achieved. [30]

4.2 Non-Relativistic QCD

In LQCD, quark masses are given in lattice units $m_q a$, such that finer lattices require smaller values of quark mass than courser lattices. When examining heavy systems with large quark masses $m_Q a$ (where $Q = b, c$ for example), the corresponding discretisation errors will remain too large at most accessible lattice spacings. For context, when dealing with b-quarks (with a rest mass of around 5GeV or $4 \cdot 10^{15} m^{-1}$ at the energy scale of the quark itself[9]), acquiring a reasonable discretisation error requires that $m_b a$ should be less than 1 such that the lattice spacing should be less than 0.04fm, which is very challenging and expensive to achieve. However, b quarks have been handled on very course lattices ($a = 0.1$fm) [2] by applying non-relativistic field theories. This has been done by incorporating the assumption that the mass of such heavy hadrons is significantly larger than the differences in mass of the different excitation states of the hadron. These differences are similar for systems containing b and c quarks, suggesting a common mechanism for these excited states, as well as reflecting kinetic energies of the quarks within these hadrons to be of the order of a few hundred MeV up to a GeV. This energy scale is somewhat larger than (if not approximately equivalent to) that of light quark systems, nevertheless being much smaller than the mass of the heavy quarks themselves. The internal momenta of the b and c quarks are thus considered to be small compared to their mass, so the quark action can be formulated accurately by assuming non-relativistic behavior [30]. In the context of LQCD, this

[9] Conversion factor: $1eV \approx 8 \cdot 10^5 m^{-1}$

is often done with the effective field theory Non-relativistic QCD (NRQCD) or the Fermilab formalism [2]. These methods do introduce additional substantial errors (labeled matching errors), which are conveniently absent in certain ratios of quantities such as decay constant ratios (3.4.1).

4.3 Highly Improved Staggered Quark

Another frequently used technique when simulating quarks on the lattice is the act of staggering quarks. Staggering quarks is the action of splitting and spreading out the quark fields over multiple sites of the lattice. It has been utilized as a form of discretising the quark action for over forty years, in which the quark fields are staggered on a discrete lattice structure. Staggering quarks is the quickest method to discretise in a simulation. However, naively staggering quarks (by merely introducing a discrete derivative in the Dirac action [32]) leads to the rise of the fermion doubling problem, which creates a second quark for every quark simulated per dimension. When naively attempting to stagger one quark, sixteen pairs of quarks (labeled *tastes*) are simulated on the four-dimensional lattice of LQCD (2^D), which introduce interaction effects that are accompanied by unusually large discretisation errors (proportional to a^2). These two issues are reduced significantly when utilizing the Highly Improved Staggered Quark (HISQ).

HISQ reduces the fifteen created copies to three by introducing an additional smearing operator which suppresses the taste changing interactions significantly. This makes the remaining four tastes much easier to account for when approaching them as a single quark[32]. HISQ also omits the dominating $\mathcal{O}(a^2)$ errors by inserting an additional correction term in the discrete derivative of the Dirac action. This introduced Naik term is namely dependant on a^2. The largest remaining errors are $O((ap_\mu)^4)$, which are negligible for light quarks, but unfortunately large for c quarks, even when assumed to be non-relativistic[10] Thus, when treating specifically c quarks with HISQ, the Naik term must be retuned by including a parameter ϵ which has expansions in $(am_q)^2$, making the term non-pertubative and able to account for the charm quark. Although this procedure does reduce the associated discretisation errors of the c quark significantly, they still remain higher than those of light quarks when utilizing the untuned Naik term correction, due to the discretization effects simply being more pronounced for the heavier quark. [1]

4.4 Heavy Quark Effective Theory

The Heavy Quark Effective Theory (HQET) is an accurate approximation for physical systems in which a stationary heavy quark interacts with particles whose four momentum is much smaller than its mass m_Q, such as for example a $(Q\bar{q})$ meson. In HQET the heavy quarks' mass m_Q is taken to be infinite, while its four-velocity v^μ is considered constant. For context, the four momentum of the light quark would be of the order of the non-pertubative scale ($p_q^\mu \sim \Lambda_{QCD}$), as a result of the fact that radius of the heavy-light meson is at least inversely this ($r \sim 1/\Lambda_{QCD}$) and the uncertainty principle that must be adhered to. If an amount of the light quarks' four-momentum $\partial^\nu p_q^\mu$ is relocated to the stationary heavy quark (with momentum $p_Q^\mu = m_Q v_Q^\mu$), the change in the heavy quarks' four velocity becomes [33]:

$$\partial^\nu v_Q^\mu \sim \frac{\partial^\nu p_q^\mu}{m_Q}. \tag{4.5}$$

Recall that our physical system is characterized by $p_q^\mu \ll m_Q$, such that the change in the heavy quarks' four-velocity $\partial^\nu v_Q \to 0$, implying a constant four velocity in the infinite mass limit. The infinite mass limit simplifies strong force interactions of the meson by introducing two symmetries. The heavy quark spin-symmetry arises due to the fact that the infinitely heavy quarks' spin decouples from the dynamics of the system, while the heavy flavour symmetry (which states that the infinitely heavy quark can be replaced by another infinitely heavy quark of different flavour without altering any other properties) is introduced due to the fact that in full QCD flavour effects are only dependant on mass [34].

Due to spin decoupling from the dynamics, the pseudoscalar and vector mesons are indistinguishable in the infinite mass limit, and their decay constant ratio equates to one up to pertubative corrections. This is especially practical in Lattice QCD calculations when the heavy quark is allowed to propagate through the entire space-time lattice, unrestricted by any artificial constraints, imitating physical systems relatively accurately. This way the physical heavy-quark masses can be interpolated (to points corresponding to $1/m_Q$) instead of extrapolated [35].

[10] To quantify this: when dealing with a fine lattice spacing a of $0.06fm$ and consequently a c quark mass $m_c a$ of approximately 0.6, the discretisation errors $O((m_c a)^4)$ will still be above the order of 10 percent!

4.5 Key missing effects

LQCD, together with the many techniques developed to accurately describe and predict the behaviour of quarks and gluons within hadrons, incorporates the strong force better than no other non-pertubative model. In unravelling the underlying processes, it can often accurately predict the behaviour and properties of particles undergoing weak interactions as well (3.4). However, LQCD fails to incorporate numerous physical effects, one of them being the electromagnetic force.

4.5.1 Electromagnetism

Although significantly weaker than the strong force at non-pertubative energy scales, electromagnetic effects would take form in slight discrepancies from the derived values when compared to the real-world system they represent. The mass of the $B^+_{(c)}$ mesons, for example, would be determined through LQCD to be lower than the true physical value, since the positive charges of the quarks composing the meson would contribute to an electromagnetic repulsion within the system, necessitating a higher effective binding energy between the quarks than predicted by LQCD. This effect can be quantified as an equation [1]:

$$M(Qq) \approx M(Qq)_{LQCD} + Ae_Qe_q + Be_q^2 + C(m_q - m_l) \tag{4.6}$$

Here A represents the strength of the Coloumb interaction, B the strength of the light quarks self-energy effect[11], while the C term accounts for the difference in mass between the possible valence u or d quark within the meson. From experimental values of neutral and charged B and D mesons, values of $A \approx 4$MeV, $B \approx 3$Mev and $C \approx 1$ were found. It is noteworthy to mention that even though the u and c quark both have the same positive charge, the resultant effect of EM is not equivalent for the B^+ and B_c^+, due to the last term in equation 4.6. Electromagnetic effects also have an impact on the decay constant of the mesons, though not as clear-cut as for the effective mass. Due to the repulsive behaviour of the quarks within the real-world meson, the magnitude of the overlap of the meson state with the vacuum state (equation 3.4) would be larger[12], resulting in a higher value of the product $f_{B^+_{(c)}} M_{B^+_{(c)}}$ than that determined through LQCD. However, due to the increased effective binding energy associated with this introduced repulsion (and thus higher effective mass $M_{B^+_{(c)}}$), both the denominator and numerator of the expression for the decay constant[13] increase, with no clear shift towards an increase or decrease of $f_{B^+_{(c)}}$ immediately apparent.

4.5.2 Charm quarks in the sea

Another key contributing factor for the $B^+_{(c)}$ decays that is often not taken into account in LQCD calculations so far is the effects of c quarks in the sea, which are the consequence of the c quarks self-energy contributions[14]. Whether the c sea quark self energy would contribute positively or negatively towards the effective meson masses isn't so clear cut. An argument for a positive contribution towards the meson mass is through the assumption that the c sea quarks self energy and mass would contribute towards the system, increasing its total mass. The process of acquiring c quarks in the sea is namely through massless gluons annihilating to massive c quarks and anti-quarks, for an instant making the inner structure of the meson look like a four particle system (if only considering the valence quarks and one pair of produced c sea quarks). This is, however, a too simplistic approach. A better interpretation of the effects of the c quark in the sea is by considering that the continuous exchange of gluons is what actually holds the meson together, and that the lack of high momentum gluons (which is due to their momentary creation of such heavy c quark anti-quark pairs) reduces the attraction between the valence quarks, requiring a higher binding energy for the systems stability. Thus the c quarks in the sea ultimately cause an attractive force (signifying that its effects also reduce the mesons decay constant), which can be visualized by their pertubatively estimated correction to the potential [1]:

$$V(r) = -\frac{C_f\alpha_s}{r} \rightarrow -\frac{C_f\alpha_s}{r}(1 + \frac{\alpha_s r}{10m_c^2}\delta^3(r)) \tag{4.7}$$

[11] This self-energy effect term is not relevant for Q since it is already absorbed in the heavy quark mass.

[12] A simplified interpretation of this is that the meson "is more eager to decay" under these circumstances.

[13] $f_{B^+_{(c)}} = \frac{\langle 0 | J_{A_0} | B^+_{(c)} \rangle}{M_{B^+_{(c)}}}$

[14] Self-energy is not inherent to the particle itself, but acquired through the interactions of the particle and the system it is a part of.

The c sea quark effects only contribute significantly to the B_c^+ meson mass and not to the B^+ mass due to the fact that the quark states of the B_c^+ are much more sensitive to these high momentum gluons (that are able to generate the virtual $c\bar{c}$ pairs) [1] (The c quarks in the sea will however effect both the mesons decay constants).
However, if the self-energy effects of c quarks in the sea contribute significantly enough towards the mass of B_c^+, wouldn't the self-energy contributions of u sea quarks contribute towards the B^+ mass in the same manner? They *do*, but due to their low mass, the continuous flickering of light quarks in the quark sea (corresponding to relatively low momentum gluons) is nearly negligible for the inner structure of any system, whether its of the B_c^+ or the B^+ [22].

Despite the effects of c sea quarks often being absent in simulations on the lattice due to their considerable computational demand, recent simulations have been able to include their effects. In these cases, the inclusion of different quarks in the sea is denoted by N_f, which indicates the number of flavours simulated with respect to their mass hierarchy. The most common configurations of sea quark inclusion are $N_f = 2$ (only incorporating the u and d quarks), $N_f = 2 + 1$ (incorporating the u, d and heavier s quarks) and $N_f = 2 + 1 + 1$ (incorporating the u, d, s and even heavier c quark).

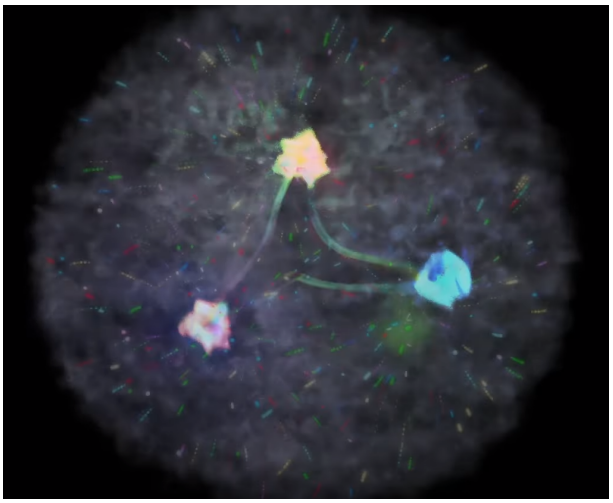

Figure 4.2: A simplified visualisation of the valence quarks and quark sea within a proton [36].

5 The parent mesons B^+ and B_c^+

The B^+ meson consists of a $\bar{b}$ and a u quark, naturally classifying itself within the category of heavy-light mesons (mesons that are composed of a heavy and a light quark as described in figure 3.2). A fascinating aspect of this family is the in-medium effects which mildly contribute towards the meson properties (when compared to light-light mesons)[37]. The in-medium effects (present at high energy collisions such as heavy-ion collisions and proton-proton collisions at the LHCb) represent the impact of the nuclear medium, including, for example, the higher particle density (when compared to vacuum) leading to the interaction of the mesons with nucleons and other particles present in the medium[38]. These effects should contribute positively towards the weak decay constants and negatively towards the meson mass (thus can be considered as an effective repulsive force within the meson). These effects arise due to the partial restoration of chiral symmetry in the presence of the nuclear medium (Vaccuum -the absense of particles- namely breaks this symmetry).

The second parent meson taken into consideration is the B_c^+, which is the heaviest meson that decays purely via the weak interaction[39]. If only taking into consideration that this meson consists of a $\bar{b}$ and a c quark, one would naively categorize the B_c^+ meson as heavy-heavy. There is, however, more to examine regarding the classification of this meson than just the masses of its constituent quarks. On the one hand, when considering the in-medium effects, which are even more negligible for this meson than for the heavy-light group -due to the weaker coupling of its heavier quarks to the medium[37]- its placement with heavy-heavy mesons seems more promising. On the other hand, when regarding the windows of the approximate chiral spin symmetry $(SU(2)_{cs})$[15] for mesons containing the charm quark, they exhibit analogous behaviour to light mesons [40]. This indicates that (to a certain extent) B_c^+ distinguishing left- and right-handed particles and undergoing spin transformations is similar to heavy-light mesons undergoing the same processes. A more detailed discussion regarding the placement of the B_c decay constant ratio, which indicates that this meson exhibits characteristics from both the heavy-heavy and heavy-light groups, is given in 6.4.

6 Results

The decay property that is the focus of this comparative analysis (namely the decay constant $f_{B^+_{(c)}}$) is extracted from Lattice QCD simulations while being multiplied by $\sqrt{M_{B^+_{(c)}}}$ (equation 3.10). It is for this reason that first the LQCD determined $B^+_{(c)}$ meson masses are considered, before analysing the LQCD decay constants. The determination of the decay properties of mass and decay constant utilized the different approaches (and combinations of them) as was elaborated on in section 4.

6.1 Mass M_{B^+}

NRQCD b quarks and HISQ c quarks

A determination of the B^+ meson mass is done in ref. [1] by utilizing its valence b quark to be in the NRQCD formalism and its u quark in the HISQ formalism. A $N_f = 2 + 1$ configuration was utilized and the lattice spacings a were of determined values around 0.09, 0.11 and 0.15 fm. The justification for using NRQCD b quarks is due to its velocity $v_b \approx 0.01c$, while its lighter partner quark with $v_u > 0.4c$ required to be considered with a relativistic formulation. The determination of the mass of B mesons was done by comparing the one-b-quark-containing B meson to a reference state containing one or two b quarks:

$$M_B = (E_B - \frac{1}{n}E_{ref})a^{-1} + \frac{1}{n}M_{ref} \tag{6.1}$$

Here E_B and E_{ref} are determined on the lattice of spacing a, M_{ref} is the experimental value of the reference state and n indicates the number of b quarks present in said reference state. To acquire relatively low uncertainty (originating the a^{-1} term), the reference state should be chosen such that $(E_B - \frac{1}{n}E_{ref})$ is as small as possible. Due to the absence of such a suitable reference state for the B^+, its mass was determined indirectly in this article by evaluating its difference to the B_s $(\bar{b}s)$ meson mass in order to avoid these large uncertainties. The reference state used for the determination of the B_s mass was the bottomonium $(b\bar{b})$, such that equation 6.1 becomes:

$$M_{B_s} = (E_{B_s} - \frac{1}{2}E_{b\bar{b}})a^{-1} + \frac{1}{2}M_{b\bar{b}} \tag{6.2}$$

[15] $SU(2)_{cs}$ is the symmetry group that includes the transformations of both spin and chirality.

The relevant values for the LQCD determined energies can be found in figure 9.1 in the appendix, while the tuned value of $M_{b\bar{b}}$ was found to be 9.450(5)GeV (this value purposefully does not take EM effects into account, such that it is compatible with the other LQCD determined values.)[1].

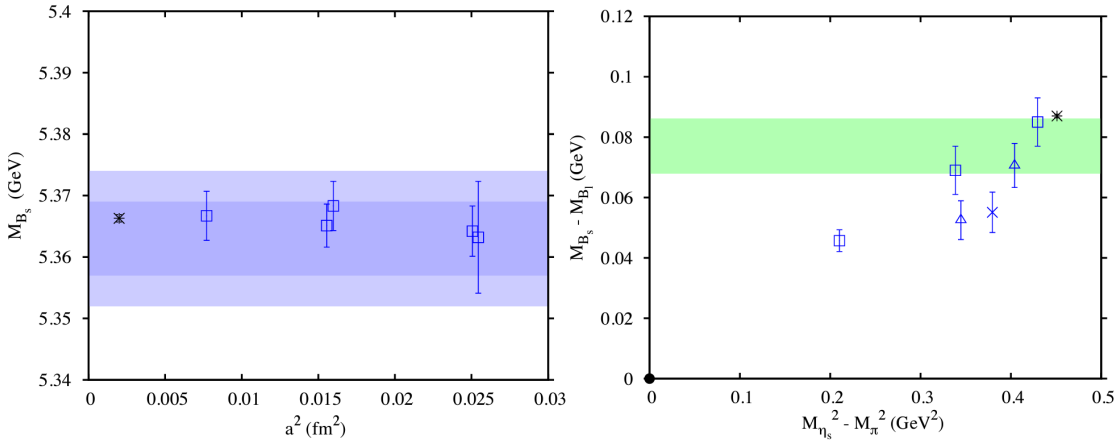

Figure 6.1: Values of the B_s mass for different lattice spacings and $M_{B_s} - M_{B^+}$ for the determination of M_{B^+}. There are multiple values for a single lattice spacing due to multiple values taken for the c quark mass to account for mis-tuning errors. The light shaded blue band indicates the associated systematic and statistical error of the determined B_s mass, while the dark shaded blue and green bands indicate the missing effects of EM, as determined by equation 4.6.[1].

Extrapolating the B_s mass which corresponds to zero lattice spacing, a value of $M_{B_s} = 5.363(6)(9)$GeV is found, indicated by the black cross in figure 6.1 (which is shifted from $a^2 = 0$ for clarity within the graph). The first uncertainty is statistical due to lattice spacing term and the second is systematic due to the NRQCD formulation of the b quark and when combined[16] give $M_{B_s} = 5.363(11)$GeV. Using this value to determine the B^+ mass is done by finding the relation between $M_{B_s} - M_{B^+} (= (E_{B_s} - E_{B^+})a^{-1})$ and ${M_{u\bar{s}}}^2 - {M_{u\bar{u}}}^2$ (which correspond accurately to $\frac{1}{2}({m_s}^2 - {m_u}^2)$). Extrapolating what the value of $M_{B_s} - M_{B^+}$ would be at ${M_{u\bar{s}}}^2 - {M_{u\bar{u}}}^2 (\approx \frac{1}{2}({m_s}^2 - {m_u}^2)) = 0.45$GeV, gives a value of 0.073(14)GeV. According to equation 4.6, the effects of electromagnetism will shift this value down by 1.3(7)MeV. This shift due to electromagnetism is calculated according to ref. [41] (which is where ref. [1] obtained equation 4.6). It differs from the 1MeV shift in [1] by accounting for $1/m_b$ effects and other limitations of equation 4.6 in the form of a 50% error on the shift. Including this shift gives us $M_{B_s} - M_{B^+} = 0.072(14)$GeV. Therefore we can find the mass of the B^+ meson to be $M_{B^+} = 5.363(11) - 0.072(14) = 5.291(18)$GeV.

When comparing this to the experimental value of M_{B^+}: 5.27941(7)GeV[42], it is apparent that the theoretically determined value and its associated error is larger, while still incorporating the experimental value within its error. This deviation of about 12MeV, as well as the factor 10^2 increase in error can be attributed to the complex process of the simulated mass determination, which involved two extrapolations due to the absence of a suitable reference state. It can also be explained by considering that, although the NRQCD and HISQ formulations are well justified in this situation, they remain an approximation of the more complex physical system (in which e.g. the b quark is slightly relativistic[17]). The in-medium effects could also play a role in this deviation, though the magnitude of their contribution is unknown (besides that it is larger for M_{B^+} than for $M_{B_c^+}$).

6.2 Mass $M_{B_c^+}$

hh method

Ref. [1], which determined the B^+ meson mass with NRQCD b quarks and HISQ c quarks also did so

[16] The combined error is calculated with the root sum squared method: $\sqrt{0.006^2 + 0.009^2} = 0.011$.

[17] However, this example of including the dynamics of the b quark (due to it's slightly relativistic nature) would actually increase the LQCD determined mass, resulting in an even larger deviation. It is given to sketch the presence of more complexity within the physical system than the one simulated in LQCD.

for the B_c^+ meson[18], now with a retuned Naik term for the HISQ c quark (4.3). As a reference state, a linear combination of the bottomonium ($b\bar{b}$) and charmonium ($c\bar{c}$) state was chosen (to minimize the errors originating from the a^{-1} term) such that equation 6.1 becomes[19]:

$$M_{B_c^+} = (E_{B_c^+} - \frac{1}{2}(E_{b\bar{b}} + M_{c\bar{c}}))a^{-1} + \frac{1}{2}(M_{b\bar{b},phys} + M_{c\bar{c},phys}) \tag{6.3}$$

Determining the B_c^+ mass with this particular reference state is known as the *hh method* (heavy-heavy method), for which the errors associated with the calculated values of $M_{B_c^+}$ per lattice spacing (figure 9.2) are extraordinarily small, due to the term $(E_{B_c^+} - \frac{1}{2}(E_{b\bar{b}} + M_{c\bar{c}}))$ being very close to zero. Extrapolating the value of the mass of B_c^+ at zero lattice spacing gives us 6.279(10)GeV (as indicated in figure 6.2), in which almost half is the discretisation error (of 4.2 MeV) that originated from the HISQ action on the c quark (due to an assigned error of 200% for tuning uncertainty of the c quark mass). Incorporating an upward shift of 1.2(6)MeV due to electromagnetic repulsion (as determined through equation 4.6) and a downward shift of 1(1)MeV because of the attraction due to c quarks in the sea (as illustrated in 4.5.2), results in a determined value of $M_{B_c^+} = 6.279(11)$ with the hh method. Note that the effects of electromagnetism canceled out with the effects of c quarks in the sea in this determination, such that they are only observed in the final value of $M_{B_c^+}$ as a slightly larger associated error.

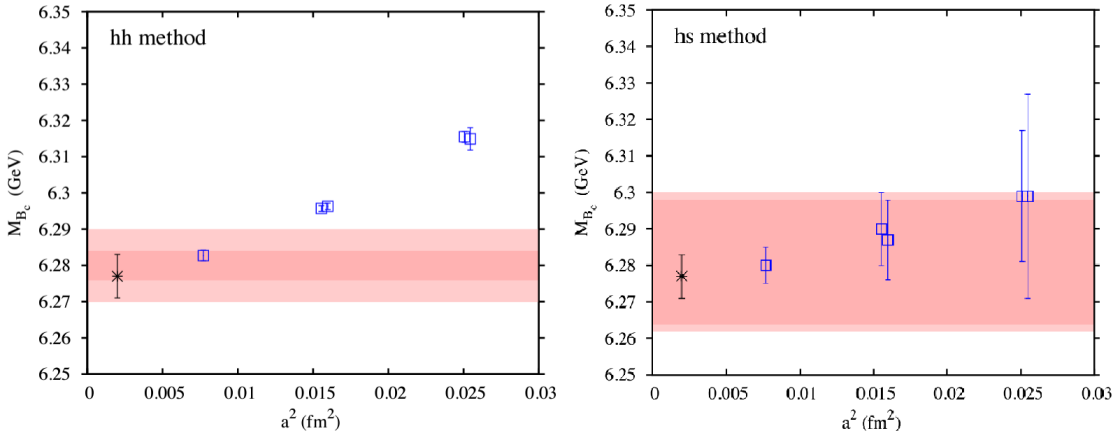

Figure 6.2: Values of the mass of B_c^+ for different lattice spacings for both the hh and hs methods. The dark shaded bands indicated missing EM effects. [1]

hs method

Still using NRQCD b quarks and HISQ c quarks, a reference state that is a superposition of the B_s ($b\bar{s}$) and the D_s^+ ($c\bar{s}$) can be chosen to determine $M_{B_c^+}$ (known as the *hs method*), such that equation 6.1 becomes:

$$M_{B_c^+} = (E_{B_c^+} - (E_{b\bar{s}} + M_{c\bar{s}}))a^{-1} + (M_{b\bar{s},phys} + M_{c\bar{s},phys}) \tag{6.4}$$

Extrapolating the value of $M_{B_c^+}$ at zero lattice spacing by tuning the NRQCD b quark (with assigned tuning error of 50%) and HISQ c quark (with a tuning error of 200%), a value of 6.280(19)GeV is acquired. This value has already incorporated the upward shift of 1.2(6)MeV due to electromagnetism and the downward 1(1)MeV shift due to the effects of c quarks in the sea.

HISQ b and c quarks

Ref. [2] uses the HISQ action for both the c and b quark, utilizing the $N_f = 2+1$ configuration and simulations of lattice spacings between 0.044 and 0.15fm. The mass of B_c^+ (which is considered an antisymmetric heavyonium state of $c\bar{b}$) was determined through its difference in binding energy between the mass of the symmetric heavyonium states $\eta_c(c\bar{c})$ and $\eta_b(b\bar{b})$:

$$\Delta_{H_c,hh} = M_{H_c} - \frac{1}{2}(M_{\eta_c} + M_{\eta_b}) \tag{6.5}$$

[18]The justification for this is due to $v_b \approx 0.04c$ while $v_c \approx 0.35c$ for B_c^+.
[19]$n = 2$ since our chosen reference state still contains two b quarks.

This term is comparable to the reference state term of equation 6.1 and is also desirably small for the same reason (for small corresponding uncertainties from the lattice spacing a^{-1}). M_{B_c} is reconstructed by evaluating this term up to the physical b mass (such that $H = B$). The result of this (derived from the multi-exponential fit) is $\Delta_{B_c,hh} = 0.065(9)$GeV, as can be seen in figure 6.3.

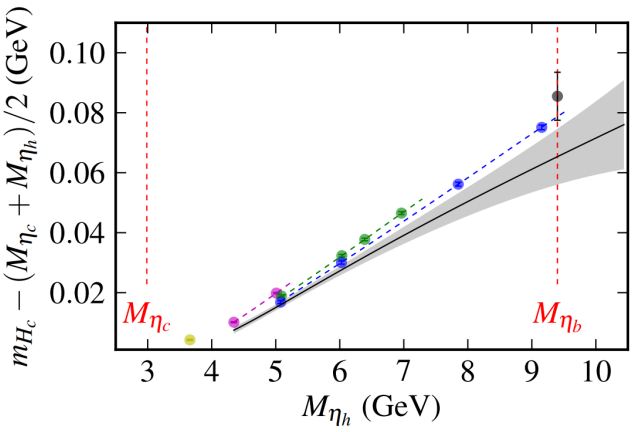

Figure 6.3: Results of expression 6.5 as a function of the heavionium mass M_{η_h} for different ensembles on the lattice (indicated by the different colours). The multi-exponentional fit resulting from this is plotted as the black line, and the value of $\Delta_{B_c,hh}$ obtained is the fit function evaluated at the physical b mass (at M_{η_b}). [2]

The LQCD derived value of $\frac{1}{2}(M_{\eta_c} + M_{\eta_b}) = 6.186(2)$GeV, such that $M_{B_c^+} = 6.251(9)$GeV. Although the effects of EM were supposedly derived in this article with the same calculations as for the previous two B_c^+ mass determinations[20], the effects do have inexplicably large varying values. The EM effects increase the determined mass by a comparable factor (3.1MeV), while the c quark in the sea effects *increase* the mass by a staggering value of 5.3MeV. Not only is the effect of increasing the mass (instead of decreasing it) a huge deviation from the previously calculated effect of the c sea quarks, but the value itself is a factor of five times larger. Taking these determined effects into account, a value of $M_{B_c^+} = 6.259(12)$GeV is acquired through this determination method, while if the effects as were determined in ref. [41] are taken into account, a value of $M_{B_c^+} = 6.251(10)$ would be acquired. This latter value is the one we will consider further.

When compared to the experimentally obtained value of $M_{B_c^+} = 6.27447(32)$ [42], an evident decrease in value is observed (while all other mass determinations exhibited a larger value when compared to experiment). This deviation of 23MeV is not incorporated in the determined associated error, casting significant doubt on the reliability of this result.
On the other hand, comparing the (NRQCD b, HISQ c) hh and hs determined masses with the experimentally obtained $M_{B_c^+}$ results in the smallest deviation so far (around 5MeV).

Determined Meson Masses in GeV				
Meson	NRQCD b and HISQ c [1]	HISQ b and c [2]	Averaged mass	Experimental value[42]
B^+	5.291(18)	-	5.291(18)	5.27941(7)
B_c^+	6.279(11), 6.280(19)	6.251(10)	6.279(10)*	6.27447(32)

Table 6.1: Table of determined and averaged meson masses, with the relevant articles cited. The averaged mass was determined through the weighted average of the LQCD values. **It was decided to not take $M_{B_c^+}$ determined with HISQ b and c quarks into account due to its questionable reliability and such that the comparison to M_{B^+} could be done on equal footing (only determined through NRQCD b and HISQ c quarks).*

The weighted average of the determined masses is denoted to encapsulate all findings discussed so far in a single value (such that it can be utilized to determine the branching fraction in section 6.5), as well as to

[20] When mentioning and having determined the relevant missing effects, ref. [2] referred to [1].

acquire a smaller associated uncertainty. If the HISQ b and c quark determination is taken into account in the weighted average of $M_{B_c^+}$, a value of 6.271(8)GeV is obtained. Although this is closer to the experimental value (as well as having a smaller associated error) than the weighted average denoted in table 6.1, this paper will continue to recognise the latter due to the scepticism surrounding the HISQ b and c quark determined mass.

The deviation in values, but more significantly the much larger associated uncertainty of all the LQCD-determined masses with respect to the experimentally obtained ones exhibited in table 6.1 raises the question: *Why determine properties of hadrons with LQCD at all, when these values can be determined experimentally with better precision and accuracy?* A straightforward answer is that not all these properties are possible to determine (directly) through experiment at this stage (such as the decay constant) thus necessitating theoretical determination methods. It is also the case that many experimental results deviate from SM model predictions greatly (deviations larger than 5σ for example point towards new physics). Therefore, a more convincing answer to our question is that the confirmation of established physics (such as the SM) as well as the search for new physics requires a collaborative effort between experiment and theory [43]. Besides this, LQCD provides an independent crosscheck of experimental values (and vice versa) for which the discrepancies can indicate effects not taken into account in theory, such as, for example, possible contributions of the nuclear medium. In the case of the meson masses considered here, the LQCD determined values were considered instead of the more precise experimental ones in order to asses the expression of the decay constant extraction 3.10 within the same theoretical framework.

The averaged values (as well as most of the LQCD determined ones used as input for this average) show a larger uncertainty for the B^+ than for the B_c^+. This goes against expectations, since the B_c^+ has errors associated to it in LQCD that are absent for the B^+. The approach of utilizing HISQ c quarks (done in both determinations of $M_{B_c^+}$) namely requires retuning the Naik term, whose associated errors are larger than for the untuned Naik term in the case of the lighter u (and in this case also s) quark. The determination of the B_c^+ mass also needed to incorporate the effects of c quarks in the sea, along with its corresponding 1MeV uncertainty (which was not necessary for M_{B^+}). However, this effect ended up canceling with the effects of EM nicely, such that their only contribution was a 1MeV larger uncertainty than if not taken into account at all, which is relatively low compared to the large uncertainty of the B^+ mass. This relatively larger error for M_{B^+} can be partially justified by the absence of a suitable reference state in it's determination and the absence of multiple LQCD determined B^+ masses that could lower the associated error for the weighted averaged mass (as was done for the B_c^+ averaged mass).

6.3 Decay constant f_{B^+}

The Flavour Lattice Averaging Group (FLAG) [13] gives an overview of lattice results so far, in which four determined values of the B^+ meson decay constant have been reviewed. In the $N_f = 2 + 1$ configuration, two f_{B^+} values of 195.6(14.9)MeV and 197(9)MeV were found, while in the $N_f = 2 + 1 + 1$ configuration values of 184(4)MeV [4] and 189.4(1.4)MeV [5] were obtained. From this it can be confirmed that including the effects of c quarks in the sea indeed results in a reduction of the mesons decay constant, as explained in 4.5.2. Only the $N_f = 2 + 1 + 1$ decay constants are considered in this paper, since they encompass the significant c quarks in the sea effects.

NRQCD b quarks and HISQ c quarks

Ref. [4] determined the B^+ decay constant using NRQCD valence b quarks and HISQ u quarks on lattice spacings a of 0.09 to 0.15fm. After having fitted the $J_0^{(0)}$ and $J_0^{(1)}$ (equation 3.6) operators simultaneously using the multi-exponential Bayesian fitting procedure [29] the amplitudes $A_{A_0} = 0.428(9)GeV^{3/2}$ and $A_{A_1} = 0.424(7)GeV^{3/2}$ were found. Together with a procedure that determined the difference in mass of B_s and B, along with their PDG masses, a decay constant of $f_B = 0.186(4)$GeV was found. This value already incorporates the downward shift due to EM effects, which were determined with 4.6 to be 1(1)MeV. To determine f_{B^+}, an extrapolation of the amplitudes to fictitious mesons of $u\overline{u}$ and $d\overline{d}$ (for distinction) was taken into account, resulting with a f_{B^+} of 0.184(4)GeV.

HISQ b and c quarks

Ref. [5] determined f_{B^+} with HISQ c and b quarks on five lattice spacings between 0.03fm and 0.12fm. This

paper also utilized a sixth lattice spacing of 0.15fm to check the estimate of discretisation errors, but didn't use it for extracting the values since its inclusion worsened the fit. This fit of $f_P\sqrt{M_P}$ evaluated at zero lattice spacing yielded a parameterization of the decay constant expression as a function of a H_s meson mass and valence light quark mass m_x.

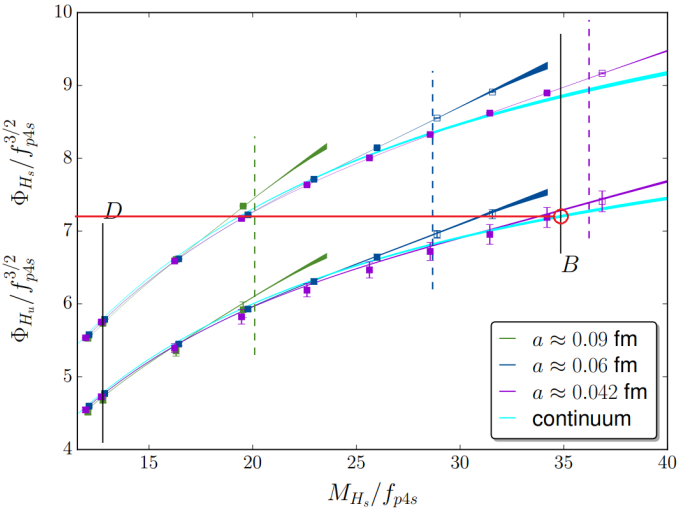

Figure 6.4: Decay constant expressions plotted in units of f_{p4s}, which is defined as a fictitious pseudoscalar meson decay constant with a valence quark of mass $0.4m_s$ (it's value has been extrapolated to be ~ 6.5GeV). The Φ_{H_u} corresponds to $f_{B^+}\sqrt{M_{B^+}}$, such that the y-axis is unitless. The two sets of data/fit lines correspond to the m_u (lower set) and m_s (higher set) valence quark mass (thus corresponding to the decay constants of B and D systems respectively). The red circle indicates the value of interest. (Adapted from [5])

For determining $f_{B^+}\sqrt{M_{B^+}}$, the M_{H_s} is taken to be M_{B_s} (with an experimental value of 5.36682(22)GeV), which is indicated by the second vertical line labelled B in figure 6.4 and the valence light quark mass is taken to be m_u, which is indicated by the lowest curve/set in figure 6.4. After incorporating the value of the B^+ mass and the effects of electromagnetism (as well as the others highlighted by the paper), ref. [5] obtains a B^+ decay constant of 0.1894(14)GeV. The preciseness of this determined decay constant can be justified by the utilized fit function that was composed of the combination of three effective field theories (including a matrix element of a HQET current) and ultimately consisted of 60 fit parameters.

Decay constant ratio

In ref. [3], the decay constant ratio (section 3.4.1) $R_l = \frac{f_{B^*}}{f_B}$, $l = u, d$ is determined on lattice spacings between 0.09 and 0.15 fm, $N_f = 2+1+1$ while using NRQCD valence b quarks and HISQ u quarks. These results are also compared to HQET expectations. The determination of the B decay constant ratio is done by analyzing its difference to the $R_s(=\frac{f_{B_s^*}}{f_{B_s}})$, due to their very similar behaviour and values. The expression used for finding $\frac{R_l}{R_s}$ is derived from equation 3.11 to be:

$$\frac{R_l}{R_s} = \left(\frac{A^{(0)}_{B_l^*} + A^{(1)}_{B_l^*}}{A^{(0)}_{B_l} + A^{(1)}_{B_l}}\right)\left(\frac{A^{(0)}_{B_s} + A^{(1)}_{B_s}}{A^{(0)}_{B_s^*} + A^{(1)}_{B_s^*}}\right) \tag{6.6}$$

Here the values can be determined with the multi-exponential Bayesian fit function which is a function of a and the relevant quark masses. Using the determined values to determine and plot $\frac{R_l}{R_s}$ for different ensembles against the light quark mass in units of the physical s quark mass gives us a value very close to one[21] with a slight decrease when the light quark approaches its physical value.

[21] This is expected since this ratio indicates the difference in $SU(3)$- and spin-symmetry breaking, which should be equivalent for the two considered systems

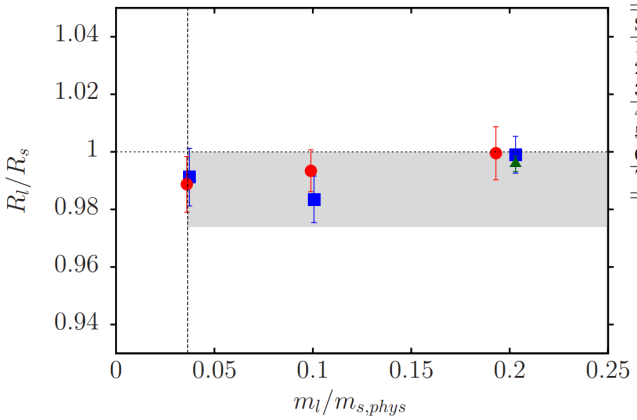

Set	$R_s^{\text{unren.}}$	$R_l^{\text{unren.}}$
1	1.0215(25)	1.0205(59)
2	1.0206(36)	1.0038(73)
3	1.0196(26)	1.0106(97)
4	1.0006(19)	1.0001(90)
5	0.9965(17)	0.9899(71)
6	0.9967(8)	0.9854(97)
7	0.9775(14)	0.9734(23)

Figure 6.5: $\frac{R_l}{R_s}$ for different ensembles against the light quark mass in units of the physical s quark mass [3].

From this, $\frac{R_l}{R_s} = 0.987(13)$. Combining this result with the found result of $R_s = 0.953(23)$ in [3], gives $R_l = 0.941(26)$ (although ref. [3] calculated this to be 0.945(26)). Taking the value of $\sqrt{\frac{M_{B^*}}{M_B}} = 1.0043$, a value of $\frac{f_{B^*}}{f_B} = 0.937(26)$ is obtained.[22]

HQET formulation

Now to compare this decay constant ratio to the purely HQET framework, for which spin dependence drops out in the infinite mass limit (section 4.4), while the renormalization factors that match the currents as described in equation 3.4 are not the same (causing a deviation for this ratio from the value of one). Evaluating a HQET expression with expansions in α_s up to $\mathcal{O}(\alpha_s^3)$ (which can be found in [3]), results in a value of $\frac{f_{B^*}}{f_B} = 0.896$, indicating a much more stable vector meson (with respect to its pseudoscalar counterpart) in a pure HQET formalism than if determined through NRQCD and HISQ valence quarks.

6.4 Decay constant $f_{B_c^+}$

NRQCD b quarks and HISQ c quarks

Ref. [3] determined the B_c decay constant using a NRQCD b quark and HISQ c quark formulation with a $N_f = 2+1+1$ configuration. Due to the radiative coefficients of equation 3.6 to be significant for the charmed B meson (see figure 9.3 in the appendix), this non-simplified form will be utilized instead of 3.7 for the multi-exponential fit function. The results of the matrix element amplitudes for the different ensembles are given in figure 6.6, along with the plotted values for $f_{B_c}\sqrt{M_{B_c}}$ per lattice spacing value a.

Set	$a^{3/2}\mathrm{A}_{B_c}^{(0)}$	$a^{3/2}\mathrm{A}_{B_c}^{(1)}$	$a^{3/2}\mathrm{A}_{B_c^*}^{(0)}$	$a^{3/2}\mathrm{A}_{B_c^*}^{(1)}$
1	0.83048(86)	-0.04792(5)	0.8022(11)	0.01541(3)
2	0.82001(45)	-0.04779(3)	0.7904(6)	0.01532(2)
4	0.58564(17)	-0.04068(2)	0.54496(22)	0.01267(1)
5	0.57350(11)	-0.04055(1)	0.53195(14)	0.01260(1)
7	0.36166(9)	-0.03158(1)	0.31990(11)	0.00941(1)

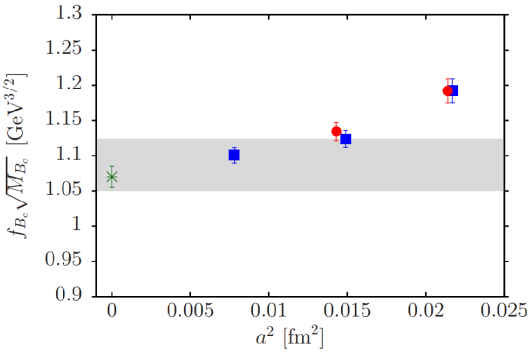

Figure 6.6: Fitted matrix element amplitudes (relevant to equation 3.6) and B_c decay constant values for varying lattice spacings. The green cross indicates the found value for previously determined decay constant using HISQ b and c quarks for comparison. [3]

[22] In ref. [3], this value deviates slightly (0.941(26)) due to the difference in calculated R_l.

Extrapolating the value of $f_{B_c}\sqrt{M_{B_c}}$ at zero lattice spacing a, gives us $1.087(37)\text{GeV}^{3/2}$, such that $f_{B_c} = 0.434(15)\text{GeV}$ [23].

HISQ b and c quarks

By evaluating both the b and c valence quarks in the HISQ formulation with a $N_f = 2+1$ configuration, ref. [2] determined the decay constant of B_c. It did this by evaluating different values of m_h (in the form of M_{η_h}) up to the physical b quark mass (this is when $h = b$) to tune the decay constant of B_c, analogous to the procedure in which the B_c meson mass was determined by evaluating $\Delta_{H_{c,hh}}$ up to the physical b mass (6.2). Plotting the results of the ensembles of the lattice spacing, along with their corresponding multi-exponential fit, results in figure 6.7, in which f_{B_c} is determined to be 0.421(6)GeV.

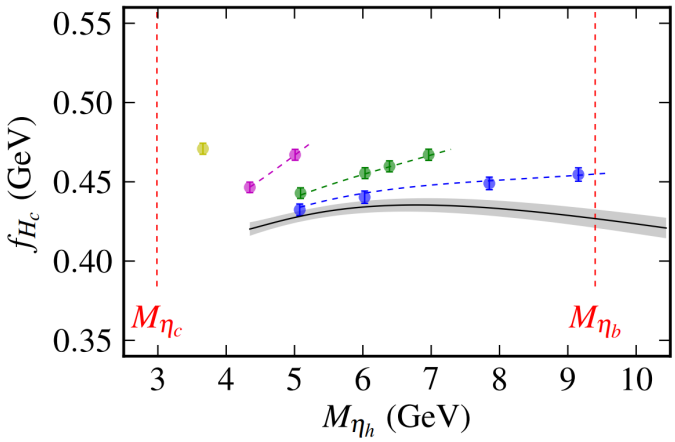

Figure 6.7: Results of f_{H_c} as a function of M_{η_h} for different ensembles, evaluated up to the physcial b mass (at M_{η_b}). The value of f_{B_c} obtained is the fit evaluated at the physical b mass [2].

Incorporating the determined EM effects (which contribute to an increase of 4(1)MeV) and the c quarks in the sea (which contribute to an increase of 2(1)MeV), we acquire a f_{B_c} of 0.421(7)GeV through the HISQ b and c quark procedure.

Meson decay constants in GeV			
Meson	NRQCD b and HISQ c [4][3]	HISQ b and c [5] [2]	Averaged decay constant
B^+	0.184(4)	0.1894(14)	0.189(2)
B_c^+	0.434(15)	0.421(6)	0.423(6)

Table 6.2: Table of determined and weighted averaged decay constants.

The results displayed in table 6.2 indicate that the uncertainty of the averaged decay constants of the B^+ is significantly lower than that of the B_c^+, which coincides with expectations, due to the present effects of retuning the Naik term for HISQ c quarks as well as including those of c quarks in the sea for $f_{B_c^+}$.

Decay constant ratio

The decay constant ratio of the axial and vector B_c mesons can be determined with the same method as for $\frac{f_{B^*}}{f_B}$, namely by comparing it to R_s. Following this procedure, a value of $\frac{f_{B_c^*}}{f_{B_c}} = 0.988(27)$ is obtained. When plotting the decay constant ratio of B_c along with those of heavy-heavy and heavy-light mesons (to analyze the internal behaviour of the mesons with respect to eachother), figure 6.8 is obtained.

[23] The weighted averaged mass of 6.279(10)GeV for the B_c was used for this determination.

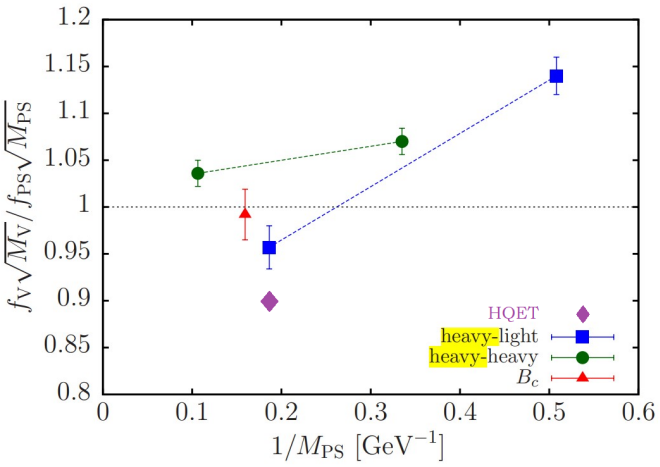

Figure 6.8: Decay constant ratio's plotted as a function of inverse mass of the pseudoscalar meson. The heavy-light data points represent the ratios $f_{B_s^*}/f_{B_s}$ and f_{B^*}/f_B (calculated in 6.3). The purple diamond is the value of the B^+ decay constant ratio obtained through HQET calculations. [3]

When considering that the LQCD-determined decay constant ratio $f_{B_c^*}/f_{B_c}$ is significantly larger than $f_{B_s^*}/f_{B_s}$ (indicated in figure 6.8) and f_{B^*}/f_B (calculated in 6.3), while also being significantly smaller than those of heavy-heavy mesons [3], one can undoubtedly confirm that the internal structure of the B_c^+ varies from both groups. In fact, when plotted, the decay constant ratio of B_c^+ lies almost perfectly in the gap between that of heavy-light and heavy-heavy mesons (with a slight "inclination" towards the heavy-light line, while also only having overlapping error bars with it). Another takeaway from figure 6.8 is that, although a family of $b\bar{c}$ mesons exist[24] of which only the B_c has been observed [2], characteristics of these unobserved charm bottom mesons are already known through such an analysis. The decay constant ratios of these mesons should namely lie between those of heavy-light and heavy-heavy and should connect to the B_c to form a line whose slope is in between those of the heavy-heavy and heavy-light.

6.5 Branching fractions of the leptonic decay modes

$\mathcal{B}(B^+ \to \tau^+\nu_\tau)$

For the determination of the branching fraction, the value of the B^+ meson mass is taken to be 5.291(18)GeV with a decay constant value of 0.189(2)GeV. A few remaining variables are required to determine the $B^+ \to \tau\nu_\tau$ branching fraction. Unfortunately, most of these have not been determined through LQCD or other theoretical frameworks yet. It is for this reason, that experimentally determined values of these variables are utilized in this branching fraction determination. B^+ has a recently theoretically determined lifetime of $\tau_{B^+} = (1.72^{+0.35}_{-0.21} \cdot 10^{-12})s$ [25] [44]. The Fermi coupling constant G_F has been determined experimentally to be $(1.1663788(6) \cdot 10^{-5})\text{GeV}^{-2}$, while the experimental mass of the tau lepton is $M_\tau = 1.77693(9)\text{GeV}$ [42]. Incorporating these values in equation 3.1, results in a SM branching fraction of:

$$\mathcal{B}(B^+ \to \tau^+\nu_\tau)^{SM} \approx 1.04(21) \cdot 10^{-4} \tag{6.7}$$

The error associated with this value was calculated with the following error propagation formula:

$$\frac{\Delta\mathcal{B}}{\mathcal{B}} = \sqrt{(\frac{\Delta\tau_{B_q^+}}{\tau_{B_q^+}})^2 + 2(\frac{\Delta G_F}{G_F})^2 + 2(\frac{\Delta|V_{qb}|}{|V_{qb}|})^2 + 2(\frac{\Delta f_{B_q^+}}{f_{B_q^+}})^2 + (\frac{\Delta m_{B_q^+}}{m_{B_q^+}})^2 + 2(\frac{\Delta m_\tau}{m_\tau^2})^2 + 2(2(\frac{\Delta m_\tau}{m_\tau^2})^2 + 2(\frac{\Delta m_{B_q^+}}{m_{B_q^+}})^2)} \tag{6.8}$$

For the value in 6.7, the error is predominantly due to the large uncertainty of the determined B^+ lifetime (since it's error was also around 20%). To analyze what relative contributions the other variables would have in the absence of this dominating error, the branching fraction of $B^+ \to \tau^+\nu_\tau$ is also determined with the

[24] This family is analogous to for example the bottomonium family (consisting of $\eta_b(NS), Y(NS)$ where $N = 1, 2, 3$ etc.) and the members of this bottom charm family would thus exhibit different spin, parity and charge characteristics than B_c^+ does.

[25] This value must be converted to $(2.61(53) \cdot 10^{12})\text{GeV}^{-1}$ before inserted in equation 3.1 such that the branching fraction is unitless. Here the relationship $\hbar = (6.582 \cdot 10^{-25})GeV \cdot s$ was utilized.

more precisely determined experimental lifetime of $\tau_{B^+} = 1.638(4) \cdot 10^{-12}$s [26]. Especially since B_c^+ has no theoretically determined lifetime yet, this is also done such that the branching fractions of $B^+ \to \tau\nu_\tau$ and $B_c^+ \to \tau\nu_\tau$ can be compared on equal footing. For these reasons, this following calculated value is what will be considered further in this paper. The branching fraction including the experimentally determined value of the B^+ lifetime becomes:

$$\mathcal{B}(B^+ \to \tau^+\nu_\tau)^{SM} \approx 0.99(6) \cdot 10^{-4} \tag{6.9}$$

The most recent branching fraction of this decay mode found experimentally by the Particle Data Group is $1.09(24) \cdot 10^{-4}$ [42]. Although the branching fraction 6.9 was determined with a combination of experimental and LQCD variables, it is compatible with the experimental measurement. Noteworthy is that the value in 6.7 (determined with a theoretically determined meson lifetime) overlaps the PDG value much more closely, which is curious since it doesn't consider the PDG given meson lifetime, while 6.9 does.

$\mathcal{B}(B_c^+ \to \tau^+\nu_\tau)$

For the determination of the $B_c^+ \to \tau^+\nu_\tau$ branching fraction, an averaged value of 6.279(10)GeV is taken for $M_{B_c^+}$, while an averaged value of 0.423(6)GeV is taken for $f_{B_c^+}$. The experimentally obtained lifetime of the B_c^+ meson is $\tau_{B_c^+} = 0.510(9) \cdot 10^{-12}$s [27] [42], causing this decays branching fraction to be:

$$\mathcal{B}(B_c^+ \to \tau^+\nu_\tau)^{SM} \approx 1.92(6) \cdot 10^{-2} \tag{6.10}$$

Since the $B_c^+ \to \tau^+\nu_\tau$ decay has not been observed experimentally, PDG does not have an experimental branching fraction to compare this value to, while also not having any upper limit for it. However, this SM branching fraction has been determined in ref. [12] to be $1.95(9) \cdot 10^{-2}$ and in ref. [10] to be $2.25(21) \cdot 10^{-2}$ with a combination of experimental and LQCD determined variables. The value given in 6.10 is very compatible with the first one, while deviating from the second greatly[28].

Comparison between the leptonic decay modes

Comparing the branching fractions determined with the experimental meson lifetimes for both decays, a very similar relative uncertainty is found, however being a factor of two times larger for the B^+ decay. This is explicable due to the fact that, although the B^+ decay has a more precise decay constant and meson lifetime, the B_c^+ decay has a smaller relative uncertainty for the LQCD determined meson mass and relative CKM matrix element. Combined, these latter variables have a larger contribution to the relative error of the branching fraction (around 35%) than the meson lifetime and decay constant (around 25%). This is represented visually in figure 6.9.

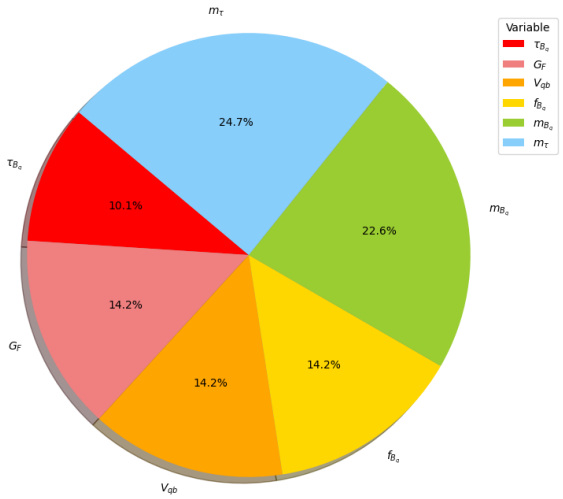

Figure 6.9: The proportional contribution of each variables relative uncertainty squared, according to equation 6.8.

[26] This corresponds to $(2.489(6) \cdot 10^{12})\text{GeV}^{-1}$.
[27] This corresponds to $(7.746(14) \cdot 10^{11})\text{GeV}^{-1}$.
[28] This is primarily due to the different derivation of the value in ref. [10], which focused on the averaged branching fraction of $\mathcal{B}(\overline{B} \to D^*\tau\nu$, which was not done for the derivation in this paper.

By incorporating the values and uncertainties of the variables in question, the contributions to the uncertainty of each decays branching fraction are represented in figure 6.10.

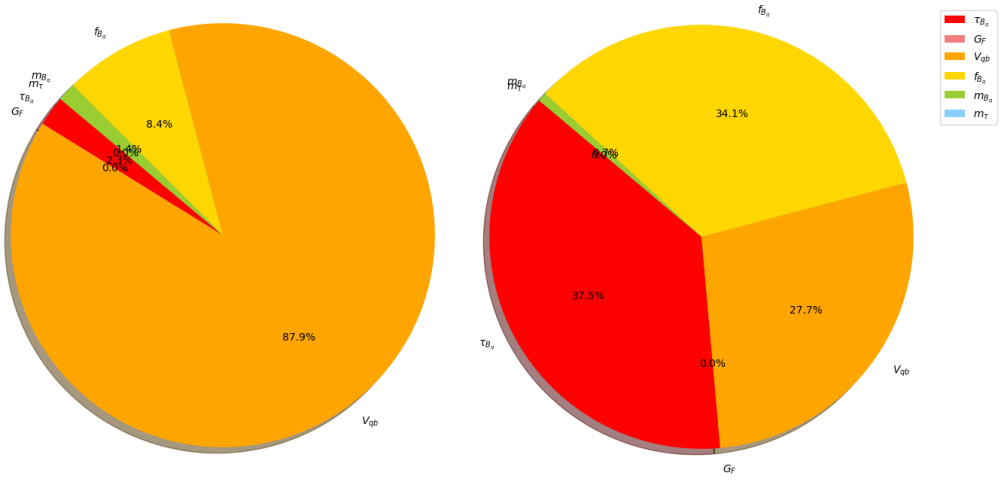

Figure 6.10: The contributions of each variables relative uncertainty squared for the $B^+ \to \tau\nu_\tau$ branching fraction 6.9 (left) and $B_c^+ \to \tau\nu_\tau$ branching fraction 6.10 (right).

As expected and assumed throughout this analysis, the CKM matrix elements and decay constants contribute most significantly over both leptonic decay modes considered. However, the most compelling finding from figure 6.9, is that the relative uncertainty squared of the B_c^+ decay associated CKM matrix element doesn't contribute predominantly as it did for the B^+ decay due to its factor ~ 3 times smaller contribution (see equation 3.3). However, this result is also the case due to the relative uncertainties of the rest of the relevant B^+ properties (decay constant, meson lifetime) being relatively low, compared to those of B_c^+, with the exception of the meson mass. The contribution of the LQCD meson mass uncertainty being so limited in figure 6.10 is due to the fact that their relative uncertainties squared were much lower than for the other variables. It must be noted that the uncertainty of the LQCD meson mass has been incorporated in that of the decay constant uncertainty though, therefore indirectly playing a more significant role than portrayed in figure 6.10.

An interesting aspect of the findings of this section is that all the branching fractions have such a low relative uncertainty when compared to the B^+ decays experimental value of $1.09(24) \cdot 10^{-4}$, while being comparable to the SM B_c^+ decay branching fraction given in [12] $(1.95(9) \cdot 10^{-2})$ and the SM B^+ decay branching fraction given in [10] $(0.858(71) \cdot 10^{-4})$. From this, it seems that the SM branching fractions when determined with the LQCD decay constant result in significantly smaller corresponding relative uncertainties than when determined experimentally, although the relative uncertainty of the B_c^+ decays branching fraction determined in [10] is particularly high, while also not agreeing with the rest of the results examined.

7 Conclusions

This comparative analysis looked at the decay properties of the leptonic decay modes $B_{(c)}^+ \to \tau^+\nu_\tau$, while investigating if and to what extent what extent those of the B_c^+ are less certain than those of the B^+ when determined through LQCD techniques. In order to asses which decay properties were most interesting the consider for this analysis, the contribution of the variables relative uncertainty towards that of the branching fractions of the leptonic decay modes were considered. Based on literature, this was expected to be the relevant CKM matrix elements and the decay constants [24]. Due to the extraction of the CKM matrix elements requiring the consideration of multiple (or all) possible final decay states (while this comparative analysis only considered $\tau\nu_\tau$), the interest shifted towards the decay constant determination through Lattice QCD. The decay constant is acquired with the square root of the meson mass when extracted through Lattice QCD (as indicated in equation 3.10), such that the LQCD determined meson masses of $B_{(c)}^+$ were considered in this analysis also.

When considering the weighted averaged meson masses, it was expected that the uncertainties would

reflect experimental data in which those of the B_c^+ decay are much larger. This was also expected by taking into consideration that B_c^+ would have errors associated to it that are absent (or smaller) for B^+. These errors are the mentioned effects of retuning the Naik term when dealing with c quarks in the HISQ formulation (4.3) and the slightly larger contribution of EM effects for the B_c^+ (equation 4.6). This was not reflected in the results, in which the averaged value of the LQCD determined masses of the B_c^+ was more precise. This outcome may be the result of the complex process of the determination of the B^+ decay properties, in which the B^+ meson state was compared to that of B_s, thus adopting all these mesons corresponding errors on top of its own discretisation errors. An improvement for this study would be to incorporate (preferably) a HISQ c and b quark determined B^+ mass in the averaged mass, such that it would (hopefully) result in a smaller corresponding error.
The values of the LQCD determined decay constants presented in this paper indeed exhibited a larger uncertainty for the B_c^+ than for B_c^+, as was expected. This can be explained by the present error of retuning the Naik term for HISQ c quarks, effects of c quarks in the sea contributing more to the B_c^+ than for the B^+ as well as the larger effect of electromagnetism for the heavier meson.
The SM branching fractions of the leptonic decay modes calculated were overall compatible with the experimental value and branching fractions determined in other papers, having values of $\mathcal{B}(B^+ \to \tau^+\nu_\tau)^{SM} \approx 0.99(6) \cdot 10^{-4}$ and $\mathcal{B}(B_c^+ \to \tau^+\nu_\tau)^{SM} \approx 1.92(6) \cdot 10^{-2}$. They were calculated with LQCD determined masses and decay constants along with experimental values for the remaining variables in equation 3.1. Ideally, the branching fraction would be determined with only LQCD determined variables (or by other theoretical frameworks) in order to compare theory to experiment and analyse the (magnitude of) deviation. However, due to the fact that many of these variables have not been determined by LQCD yet, as well as the fact that experiment doesn't offer a branching fraction (or upper limit) for the $B_c^+ \to \tau\nu_\tau$ decay, this comparison/analysis was not possible in this paper.
An evaluation regarding the overall uncertainty as well as the contributions of each variables relative uncertainty of the branching fractions was conducted in order to deduce whether the B^+ decays braching fraction was more precise than that of the B_c^+ decay. This was not the case, with the $B^+ \to \tau\nu_\tau$ branching fraction having a relative uncertainty that was twice as large. This evaluation was necessary since the decay constants (which were more precise for B^+) and the CKM matrix elements (which had a lower relative uncertainty for the B_c^+ decay) were expected to form the main sources of uncertainty in the theoretical determination of the branching fractions [13]: an indication as to their contributions highlights the regions that would benefit most from further investigation. Both leptonic decay modes (particularly the B^+ decay) would benefit greatly from a more precise determination of the relevant exclusive CKM matrix elements, while the B_c^+ decay mode would benefit greatly from a more precise determination of its parent mesons decay constant and lifetime as well.

It is for this reason, as well as because it has a significantly larger uncertainty for the B_c^+ when compared to the B^+, that a relevant decay property to investigate further within the theoretical framework of LQCD is the parent mesons lifetimes. Future studies on the subject could conclude whether the LQCD determined B^+ lifetime is more precise than that of B_c^+ (which would mirror experimental values) and an analysis on the discrepancies would enhance the knowledge regarding the parent mesons stability within theory.
The in-medium effects described in 5 were also not taken into account in any of the determined values of meson masses and decay constants, due to a lack of knowledge regarding the magnitude of their contribution. If they were taken into account, however, they should contribute to a larger uncertainty for specifically the B^+ mesons decay properties. The degree to which they would do this could also be the focus of further research on the topic.
Besides this, the B_c^+ mesons classification within the heavy-heavy/heavy-light group remains unresolved. Exhibiting behavioural aspects associated to both heavy-heavy and heavy-light mesons, some literature even went so far as to state that B_c^+ can be considered the bridge between the two [2]. However, it is important to note that the questions *To what extent is this the case?*[29] and *Do all the properties of the B_c^+ indeed exhibit the slight inclination toward heavy-light meson properties as for the decay constant ratio?* are still unanswered. This is why further investigation into the true classification of the B_c^+ meson is necessary for a more profound understanding of its intrinsic characteristics.

[29] To elaborate: *Do all properties of the B_c^+ meson fall between those of heavy-light and heavy-heavy (as indicated in figure 6.8, or are there discrepancies whose values are outliers?*

8 References

[1] E. B. Gregory, C. T. H. Davies, I. D. Kendall, *et al.*, "Precise B, B_s and B_c meson spectroscopy from full lattice QCD," *Physical Review D*, vol. 83, no. 1, Jan. 2011, ISSN: 1550-2368. DOI: 10.1103/physrevd.83.014506. [Online]. Available: http://dx.doi.org/10.1103/PhysRevD.83.014506.

[2] C. McNeile, C. T. H. Davies, E. Follana, K. Hornbostel, and G. P. Lepage, "Heavy meson masses and decay constants from relativistic heavy quarks in full lattice QCD," *Physical Review D*, vol. 86, no. 7, Oct. 2012, ISSN: 1550-2368. DOI: 10.1103/physrevd.86.074503. [Online]. Available: http://dx.doi.org/10.1103/PhysRevD.86.074503.

[3] B. Colquhoun, C. T. H. Davies, J. Kettle, *et al.*, "B-meson decay constants: A more complete picture from full lattice QCD," *Physical Review D*, vol. 91, no. 11, Jun. 2015, ISSN: 1550-2368. DOI: 10.1103/physrevd.91.114509. [Online]. Available: http://dx.doi.org/10.1103/PhysRevD.91.114509.

[4] R. J. Dowdall, C. T. H. Davies, R. R. Horgan, C. J. Monahan, and J. Shigemitsu, "B-meson decay constants from improved lattice NRQCD and physical u, d, s and c sea quarks," *Physical Review Letters*, vol. 110, no. 22, May 2013, ISSN: 1079-7114. DOI: 10.1103/physrevlett.110.222003. [Online]. Available: http://dx.doi.org/10.1103/PhysRevLett.110.222003.

[5] A. Bazavov, C. Bernard, N. Brown, *et al.*, "B- and D-meson leptonic decay constants from four-flavor lattice QCD," *Physical Review D*, vol. 98, no. 7, Oct. 2018, ISSN: 2470-0029. DOI: 10.1103/physrevd.98.074512. [Online]. Available: http://dx.doi.org/10.1103/PhysRevD.98.074512.

[6] J. O. Eeg, *Building the standard model historical and qualitative aspects*, 2022. arXiv: 2212.05501. [Online]. Available: https://doi.org/10.48550/arXiv.2212.05501.

[7] D. Tong, *The standard model of particle physics: A triumph of science*, 2021. [Online]. Available: https://www.youtube.com/watch?v=Unl1jXFnzgo&t=133s.

[8] T. Mongan, "Standard model masses explained," vol. 12, 2021. DOI: 10.4236/jmp.2021.127060. [Online]. Available: https://doi.org/10.4236/jmp.2021.127060.

[9] N. H. I Belyaev G Carboni, *The history of the LHCb*, 2021. DOI: 10.1140/epjh/s13129-021-00002-z. [Online]. Available: https://doi.org/10.1140/epjh/s13129-021-00002-z.

[10] R. Fleischer, R. Jaarsma, and G. Tetlalmatzi-Xolocotzi, "Mapping out the space for new physics with leptonic and semileptonic $B_{(c)}$ decays," *The European Physical Journal C*, vol. 81, no. 7, Jul. 2021, ISSN: 1434-6052. DOI: 10.1140/epjc/s10052-021-09419-8. [Online]. Available: http://dx.doi.org/10.1140/epjc/s10052-021-09419-8.

[11] A. Mathad, *Lepton flavour universality tests in $b \to c l \nu$ decays at the LHCb experiment*, 2023. arXiv: 2305.08133 [hep-ex].

[12] X. Zuo, M. Fedele, C. Helsens, D. Hill, S. Iguro, and M. Klute, "Prospects for B_c^+ and $B^+ \to \tau^+ \nu_\tau$ at FCC-ee," *The European Physical Journal C*, vol. 84, no. 1, 2024, ISSN: 1434-6052. DOI: 10.1140/epjc/s10052-024-12418-0. [Online]. Available: http://dx.doi.org/10.1140/epjc/s10052-024-12418-0.

[13] Y. Aoki, T. Blum, G. Colangelo, *et al.*, "Flag review 2021," *The European Physical Journal C*, vol. 82, no. 10, Oct. 2022, ISSN: 1434-6052. DOI: 10.1140/epjc/s10052-022-10536-1. [Online]. Available: http://dx.doi.org/10.1140/epjc/s10052-022-10536-1.

[14] W. Altmannshofer and N. Lewis, "Loop-induced determinations of V_{ub} and V_{cb}," *Physical Review D*, vol. 105, no. 3, Feb. 2022, ISSN: 2470-0029. DOI: 10.1103/physrevd.105.033004. [Online]. Available: http://dx.doi.org/10.1103/PhysRevD.105.033004.

[15] R. Aaij, B. Adeva, M. Adinolfi, *et al.*, "First observation of a baryonic B_c^+ *Decay*," *Physical Review Letters*, vol. 113, no. 15, Oct. 2014, ISSN: 1079-7114. DOI: 10.1103/physrevlett.113.152003. [Online]. Available: http://dx.doi.org/10.1103/PhysRevLett.113.152003.

[16] R. Aaij, C. Abellan Beteta, B. Adeva, M. Adinolfi, C. Adrover, and Affolder, "Observation of $B_c^+ \to J/\psi D_s^+$ and $B_c^+ \to J/\psi D_s^{*+}$decays," *Physical Review D*, vol. 87, no. 11, Jun. 2013, ISSN: 1550-2368. DOI: 10.1103/physrevd.87.112012. [Online]. Available: http://dx.doi.org/10.1103/PhysRevD.87.112012.

[17] R. Aaij, C. Abellan Beteta, A. Adametz, *et al.*, "Measurements of $B_c^+ \to J/\psi\pi^+ Decay$," *Physical Review Letters*, vol. 109, no. 23, Dec. 2012, ISSN: 1079-7114. DOI: 10.1103/physrevlett.109.232001. [Online]. Available: http://dx.doi.org/10.1103/PhysRevLett.109.232001.

[18] *Belle II*. [Online]. Available: https://www.belle2.org/.

[19] J. I. Illana and A. J. Cano, *Quantum field theory and the structure of the standard model*, 2022. arXiv: 2211.14636 [hep-ph].

[20] J. Romeu, "Recherche des désintégrations violant la saveur leptonique $B_s \to \tau_\mu$ et $B_d \to \tau_\mu$ avec l'expérience LHCb," Ph.D. dissertation, Sep. 2018.

[21] J. Zupan, *Introduction to flavour physics*, 2019. arXiv: 1903.05062 [hep-ph].

[22] M. O'Dowd and E. McLean, *PBS space time; did AI prove our proton model wrong?* 2023. [Online]. Available: https://www.youtube.com/watch?v=TbzZIMQC6vk.

[23] M. O'Dowd and E. McLean, *PBS space time; what happens inside a proton?* 2022. [Online]. Available: https://www.youtube.com/watch?v=WZfmG_h5Oyg&t=316s.

[24] M. Fedele, C. Helsens, D. Hill, S. Iguro, M. Klute, and X. Zuo, "Prospects for B_c^+ and B^+ to $\tau^+\nu_\tau$ at $FCC - ee$," 2023. [Online]. Available: https://doi.org/10.48550/arXiv.2305.02998.

[25] Y. Amhis, S. Banerjee, E. Ben-Haim, *et al.*, "Averages of b-hadron, c-hadron and τ-lepton properties as of 2021," *Physical Review D*, vol. 107, no. 5, Mar. 2023, ISSN: 2470-0029. DOI: 10.1103/physrevd.107.052008. [Online]. Available: http://dx.doi.org/10.1103/PhysRevD.107.052008.

[26] K. De Bruyn, "Searching for penguin footprints: Towards high precision CP violation measurements in the B meson systems," Presented 08 Oct 2015, Vrije U., Amsterdam, 2015. [Online]. Available: https://cds.cern.ch/record/2048174.

[27] D. Tong, *Quantum field theory*, 2006. [Online]. Available: https://www.damtp.cam.ac.uk/user/tong/qft.html.

[28] M. Thomson, *Handout 9 : The weak interaction and V-A*, 2011. [Online]. Available: https://www.hep.phy.cam.ac.uk/~thomson/partIIIparticles/handouts/Handout_9_2011.pdf.

[29] G. Lepage, B. Clark, C. Davies, *et al.*, "Constrained curve fitting," *Nuclear Physics B - Proceedings Supplements*, vol. 106–107, pp. 12–20, Mar. 2002, ISSN: 0920-5632. DOI: 10.1016/s0920-5632(01)01638-3. [Online]. Available: http://dx.doi.org/10.1016/S0920-5632(01)01638-3.

[30] C. Davies, *Lattice QCD - a guide for people who want results*, 2005. arXiv: hep-lat/0509046 [hep-lat].

[31] A. Bazavov, C. Bernard, C. DeTar, *et al.*, *Progress on four flavor QCD with the HISQ action*, MILC Collaboration, 2009. arXiv: 0911.0869 [hep-lat].

[32] E. Follana, Q. Mason, C. Davies, *et al.*, "Highly improved staggered quarks on the lattice with applications to charm physics," *Physical Review D*, vol. 75, no. 5, Mar. 2007, ISSN: 1550-2368. DOI: 10.1103/physrevd.75.054502. [Online]. Available: http://dx.doi.org/10.1103/PhysRevD.75.054502.

[33] M. B. Wise, *Heavy quark physics*, 1998. arXiv: hep-ph/9805468 [hep-ph].

[34] T. Mannel, *Spin effects in heavy quark processes*, 1998. arXiv: hep-ph/9803398 [hep-ph].

[35] D. Becirevic, A. L. Yaouanc, A. Oyanguren, P. Roudeau, and F. Sanfilippo, *Insight into $D/B \to \pi\ell\nu_\ell$ decay using the pole models*, 2014. arXiv: 1407.1019 [hep-ph].

[36] S. Costello, *"Visualizing the proton" through animation and film*, MIT School of Science Communications, 2022. [Online]. Available: https://arts.mit.edu/visualizing-the-proton/.

[37] A. J. Arifi, P. T. Hutauruk, and K. Tsushima, "In-medium properties of the light and heavy-light mesons in a light-front quark model," *Physical Review D*, vol. 107, no. 11, Jun. 2023, ISSN: 2470-0029. DOI: 10.1103/physrevd.107.114010. [Online]. Available: http://dx.doi.org/10.1103/PhysRevD.107.114010.

[38] M. Baldo and G. F. Burgio, "Properties of the nuclear medium," *Reports on Progress in Physics*, vol. 75, no. 2, p. 026 301, Jan. 2012, ISSN: 1361-6633. DOI: 10.1088/0034-4885/75/2/026301. [Online]. Available: http://dx.doi.org/10.1088/0034-4885/75/2/026301.

[39] *LHCb observes a new decay mode of the charmed beauty meson*, LHCb Collaboration, 2024. [Online]. Available: https://home.cern/news/news/physics/lhcb-observes-new-decay-mode-charmed-beauty-meson.

[40] T.-W. Chiu, *Symmetries of spatial correlators of light and heavy mesons in high temperature lattice QCD*, 2024. arXiv: 2404.15932 [hep-lat].

[41] C. T. H. Davies, C. McNeile, E. Follana, G. P. Lepage, H. Na, and J. Shigemitsu, "Update: Precision D_s decay constant from full lattice QCD using very fine lattices," *Physical Review D*, vol. 82, no. 11, 2010, ISSN: 1550-2368. DOI: 10.1103/physrevd.82.114504. [Online]. Available: http://dx.doi.org/10.1103/PhysRevD.82.114504.

[42] S. Navas, et al. (Particle Data Group), to be published in Phys. Rev D 110, 030001 (2024).

[43] P. Boyle, D. Bollweg, R. Brower, *et al.*, *Lattice QCD and the computational frontier*, 2022. arXiv: 2204.00039 [hep-lat]. [Online]. Available: https://arxiv.org/abs/2204.00039.

[44] J. Albrecht, F. Bernlochner, A. Lenz, and A. Rusov, *Lifetimes of b-hadrons and mixing of neutral B-mesons: Theoretical and experimental status*, 2024. arXiv: 2402.04224 [hep-ph]. [Online]. Available: https://arxiv.org/abs/2402.04224.

9 Appendix

Set	am_b	$aM_{b\bar{b}}$	$aE_{b\bar{b}}$	am_s	aM_{η_s}	aE_{B_s}
1	3.4	7.260(9)	0.27843(8)	0.066	0.52524(36)	0.6409(11)
	3.4			0.080	0.57828(34)	0.6539(10)
	3.6	7.688(5)	0.27662(7)	0.066		0.6466(13)
	3.6			0.080		0.6604(9)
	3.4($c_i \neq 1$)	7.248(4)	0.28048(7)			
2	3.4	7.261(9)	0.27902(7)	0.066	0.52458(35)	0.6417(14)
3	2.8	5.996(8)	0.28538(3)	0.0537	0.43118(18)	0.5470(15)
4	2.8	5.992(5)	0.28465(6)	0.05465	0.43675(24)	0.5527(16)
5	1.95	4.288(10)	0.25985(5)	0.0366	0.30675(12)	0.4172(10)

Figure 9.1: Relevant results for the determination of the mass of the B_s meson on different ensembles of lattice spacings (indicated by the set) for the ultimate determination of M_{B^+} [1].

Set	am_b	am_c	aM_{η_c}	aE_{B_c}
1	3.4	0.85	2.27031(16)	1.34917(27)
		0.85		
	3.4	0.88	2.32148(14)	1.37456(27)
		0.88		
	3.6	0.85		1.35415(29)
	3.6	0.88		1.37593(29)
	3.4($c_i \neq 1$)	0.85		1.34987(27)
2	3.4	0.85	2.26964(17)	1.34834(34)
3	2.8	0.65	1.84949(11)	1.11727(13)
4	2.8	0.66	1.87142(12)	1.12783(25)
5	1.95	0.43	1.31691(7)	0.81861(12)

Figure 9.2: Relevant results for the determination of the B_c^+ meson mass [1].

Set	$z_{A_0,c}$	z_1	z_2
1	-0.111(5)	0.024(3)	-1.108(4)
2	-0.105(5)	0.024(3)	-1.083(4)
4	-0.046(5)	0.007(3)	-0.698(4)
5	-0.041(5)	0.007(3)	-0.690(4)
7	-0.034(5)	-0.031(4)	-0.325(4)

Figure 9.3: Significance of the radiative effects for the determination of the B_c^+ meson decay constant ratio [3], justifying the use of equation 3.6 over equation 3.7.